Supplementary Information

Photosensitizing CNTs by organotin(IV) compounds: Generation of reactive oxygen species and degradation of Amoxicillin

Sahil Thakur[a], Jyoti Rohilla[a], Sahil Sharma[b], Raghubir Singh[b], Raman Kamboj[b], Varinder Kaur[a*]

[a]*Department of Chemistry, Panjab University, Sector-14, Chandigarh-160014, India*

[b]*Department of Chemistry, DAV College, Sector 10, Chandigarh-160011, India*

*Corresponding author: var_ka04@yahoo.co.in(V.K.)

S1.1 Synthesis of BSAL-EA

In a single-neck round bottom flask, ethanolamine (24.55 mmol, 1.50 g) was added to 5-bromosalicylaldehyde (24.55 mmol, 4.93 g) dissolved in 100 mL methanol. The reaction mixture was heated to reflux for 24 h and the contents were cooled to room temperature. The solvent was removed under a vacuum to afford a yellow solid. The product was filtered, washed with hexane and diethyl ether to remove the impurities, dried and stored under dry conditions. Yield: 90.80% (22.24 mmol, 5.43 g), Melting point: 90-92ºC; FT-IR (KBr) cm^{-1}: 3300-2950 (br, OH, intramolecular hydrogen-bonded), 1633 (C=N), 1495(C-C), 1076, 1010 (C-O), 725 (C-Br). ^{1}H-NMR (500 MHz, C*D*Cl_3): δ (ppm) 1.63 (1H, s, Alk-OH), 3.69 (2H, t, ^{3}J = 5.0 Hz, H^9), 3.85 (2H, t, ^{3}J =5.0 Hz, H^8), 6.78 (1H, d, ^{3}J =8.5 Hz, H^3), 7.30 (1H, dd, H^2), 7.32 (1H, d, H^6), 8.24 (1H, s, H^7), 13.22 (1H, s, Ar-OH); ^{13}C NMR (125 MHz, C*D*Cl_3): δ (ppm) 61.6 (C^9), 61.9 (C^8), 110.1 (C^1), 119.1 (C^3), 120.0 (C^5), 133.6 (C^6), 135.1 (C^2), 160.3 (C^7), 165.7 (C^4); ESI-MS (m/z): 244.36 $(M+H)^+$, 246.36 $(M+2+H)^+$. Anal. Calcd for $C_9H_{10}NO_2Br$ C, 44.29; H, 4.13; N, 5.74; Found: C, 44.28; H, 4.12; N, 5.76.

S1.2 Characterization of Schiff base BSAL-DAP

Melting point: 92°C. Yield: 92.30% (34.62 mmol, 3.12 g) FT-IR (ATR) cm^{-1}: 3132 (broad, OH), 2900-2800 (CH), 1629 (C=N), 1478 (C-C), 1273 (C-N), 1162 (C-O), 620 (C-Br). ^{1}H-NMR (500 MHz, C*D*Cl_3): δ (ppm) 2.11 (1H, s, Alk-OH), 3.80 (4H, m, H^8), 4.28 (1H, m, H^9), 6.86-6.88 (2H, d, ^{3}J =10 Hz, H^3), 7.39 (4H, m, $H^{2,6}$), 8.34 (2H, s, H^7), 13.08 (2H, s, OH); ^{13}C-NMR (125 MHz, C*D*Cl_3): δ (ppm) 63.22 (C^8), 70.28 (C^9), 110.30 (C^1), 119.09 (C^3), 119.98 (C^5), 133.69 (C^6), 135.35 (C^2), 160.09 (C^7), 166.30 (C^4); ESI-MS (m/z): 454.96 $(M+H)^+$, 456.96 $(M+2+H)^+$, 458.96 $(M+4+H)^+$. Anal. Calcd for $C_{17}H_{16}N_2O_3Br_2$; C, 44.76; H, 3.54; N, 6.14; Found: C, 44.32; H, 3.79; N, 6.32.

S1.3 Characterization of Sn(IV) compound 1

Melting point: 202°C. Yield: 86.87% (3.5 mmol, 1.39 g). FT-IR (ATR) cm^{-1}: 2922, 2881, 2835 (CH), 1624 (C=N), 1452 (C-C), 1052 (C-O), 778 (C-Br), 688 (Sn-C), 596 (Sn-O), 523 (Sn-N). ^{1}H-NMR (500 MHz, C*D*Cl_3): δ (ppm) 0.65 (s, 12H, $H^{10,11}$, $^{3}J(^{1}H\text{-}^{117}Sn)$ = 74 Hz, $^{3}J(^{1}H\text{-}^{119}Sn)$ =

77 Hz), 3.69 (4H, t, ^{3}J =5 Hz, H^{9}), 4.08 (4H, t, ^{3}J =5.0 Hz, H^{8}), 6.62-6.64 (2H, d, ^{3}J =10 Hz, H^{3}), 7.22 (2H, d, ^{4}J =2.5 Hz, H^{6}), 7.35-7.38 (2H, dd, ^{3}J =8.5 Hz, ^{4}J =2 Hz, H^{2}), 8.33 (2H, s, H^{7}); ^{13}C-NMR (125 MHz, C*D*Cl_3): δ (ppm) 0.15 ($C^{10,11}$), 60.26 (C^{9}), 62.58 (C^{8}), 106.87 (C^{1}), 118.49 (C^{3}), 124.82 (C^{5}), 136.05 (C^{6}), 138.90 (C^{2}), 168.30 (C^{7}), 170.51 (C^{4}); ^{119}Sn NMR (186 MHz, C*D*Cl_3): δ (ppm) −154.91; ESI-MS (m/z): 815.81 $(M+H+CH_3OH)^+$. Anal. Calcd for $C_{22}H_{28}N_2O_4Br_2Sn_2$; C, 33.80; H, 3.61; N, 3.58; Found: C, 34.34; H, 3.75; N, 3.83.

S1.4 Characterization of Sn(IV) compound 2

Melting point: 189 °C. Yield: 88.99% (1.95 mmol, 1.86 g). FT-IR (ATR) cm^{-1}: 2915, 2839 (C-H), 1633 (C=N), 1455 (C-C), 1170 (C-O), 780 (C-Br), 687 (Sn-C), 578 (Sn-O), 536 (Sn-N). ^{1}H NMR (500 MHz, C*D*Cl_3): δ (ppm) 0.59 (s, 6H, H^{17}), 0.70 (s, 6H, H^{18}), 3.74 (m, 4H, H^{8}), 4.20 (m, 1H, H^{9}), 6.62-6.64 (d, 1H, ^{3}J= 10 Hz, H^{11}), 6.84-6.86 (d, 2H,^{3}J= 10.0 Hz, H^{3}), 7.21 (d, 1H, ^{4}J=2.5 Hz, H^{12}), 7.38 (m, 5H,$H^{2,6,14}$), 8.33 (s, 2H, H^{7}), 13.39 (s, 1H, H^{16}). ^{13}C NMR (125 MHz, C*D*Cl_3): δ (ppm) 0.73 (C^{17}), 1.93 (C^{18}), 63.07 (C^{8}), 65.81 ($C^{8'}$), 72.22 (C^{9}), 107.73 (C^{13}), 110.87 (C^{1}), 119.10 (C^{3}), 119.80 (C^{5}), 120.85 (C^{11}), 125.51 (C^{15}), 134.27 (C^{6}), 135.86 (C^{2}), 136.69 (C^{12}), 139.79 (C^{14}), 161.04 (C^{7}), 166.20 (C^{4}), 171.46 (C^{10}), 196.34 (C^{16}). ^{119}Sn NMR (186 MHz, C*D*Cl_3): δ (ppm) −148.88, -465.04; ESI-MS (m/z): 950.94 $(M+H)^+$, 952.93 $(M+2+H)^+$, 954.93 $(M+4+H)^+$. Anal. Calcd for $C_{28}H_{29}N_2O_5Br_3Sn_2$; C, 35.38; H, 3.07; N, 2.95; Found: C, 35.42; H, 3.12; N, 2.65.

S1.5 Characterization of 1@CNT and 2@CNT

1@CNT: Yield: 84% (168 mg). FT-IR cm^{-1}: 2986- 2830 (C-H), 1620 (C=N), 1510 (C-C), 1049 (C-O), 769 (C-Br), 677 (Sn-C), 593 (Sn-O), 517 (Sn-N); 2@CNT: Yield: 77% (154 mg). FT-IR cm^{-1}: 2952- 2839 (C-H), 1625 (C=N), 1520 (C-C), 1103 (C-O), 782 (C-Br), 688 (Sn-C), 634 (Sn-O), 537 (Sn-N).

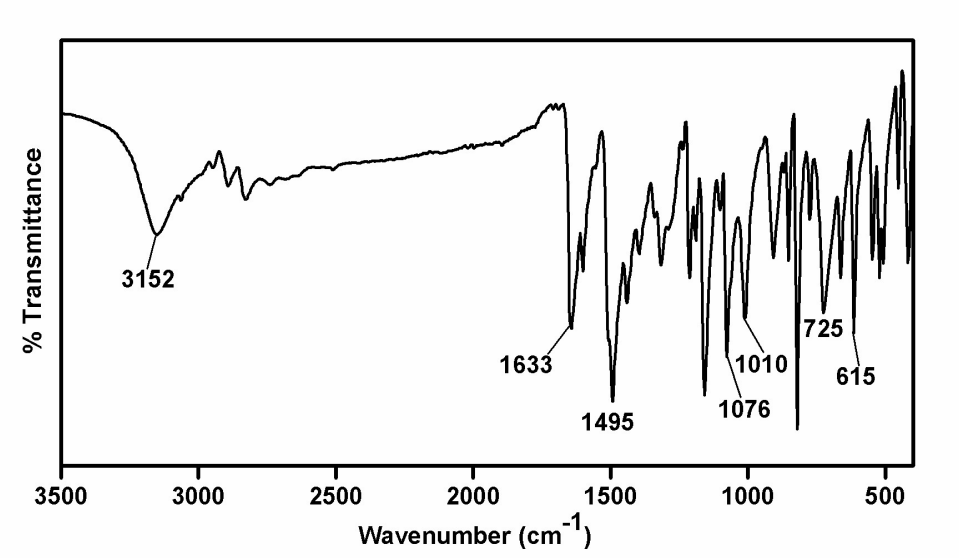

Figure S1 FT-IR spectrum of BSAL-EA

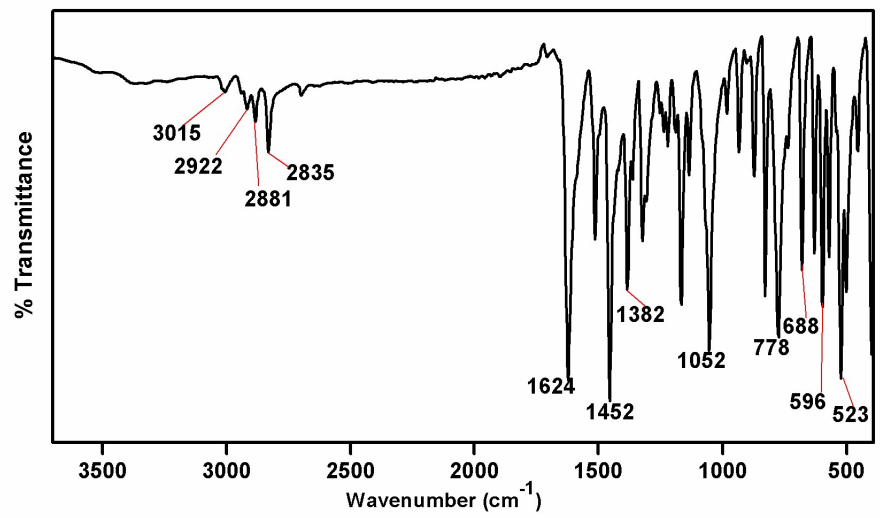

Fig. S2 FT-IR spectrum of $[Me_2Sn(SAL\text{-}EA)]_2$

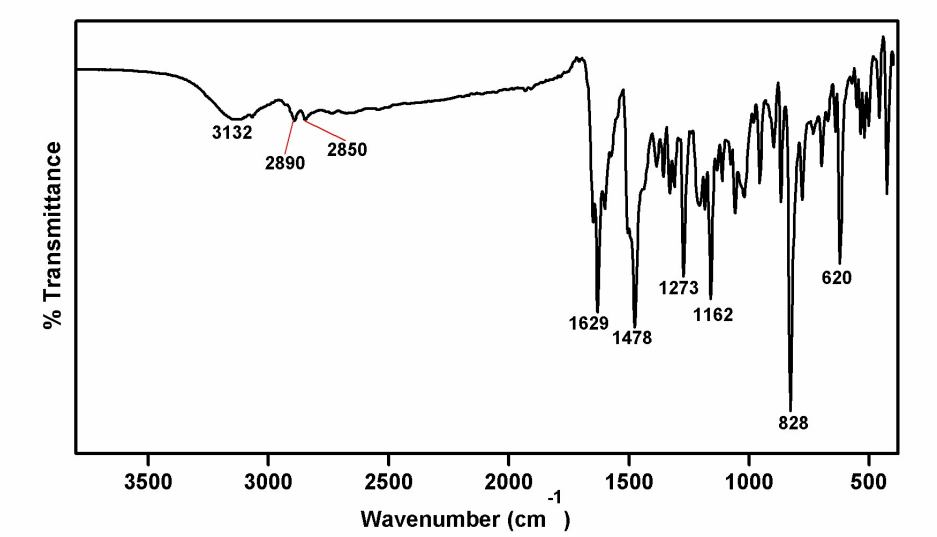

Fig. S3 FT-IR spectrum of BSAL-DAP

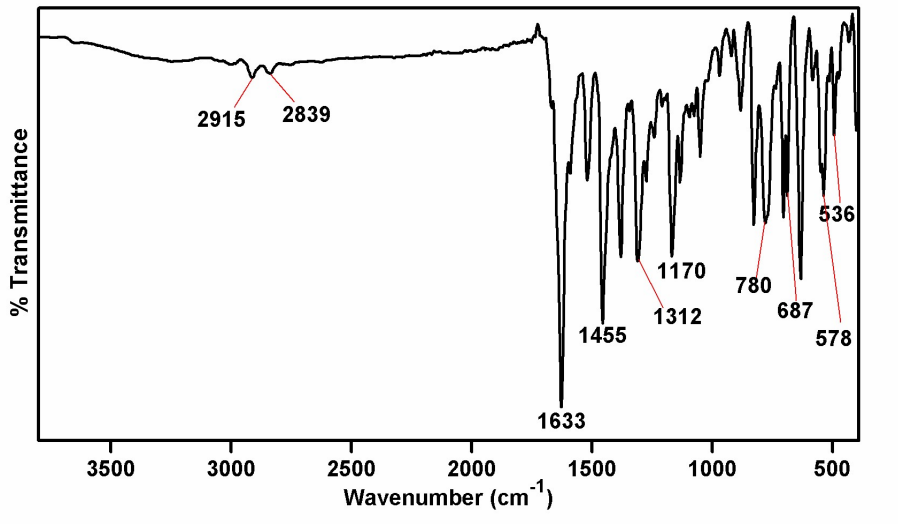

Fig. S4 FT-IR spectrum of [Me_2Sn_2(BSAL-DAP)(BSAL)]

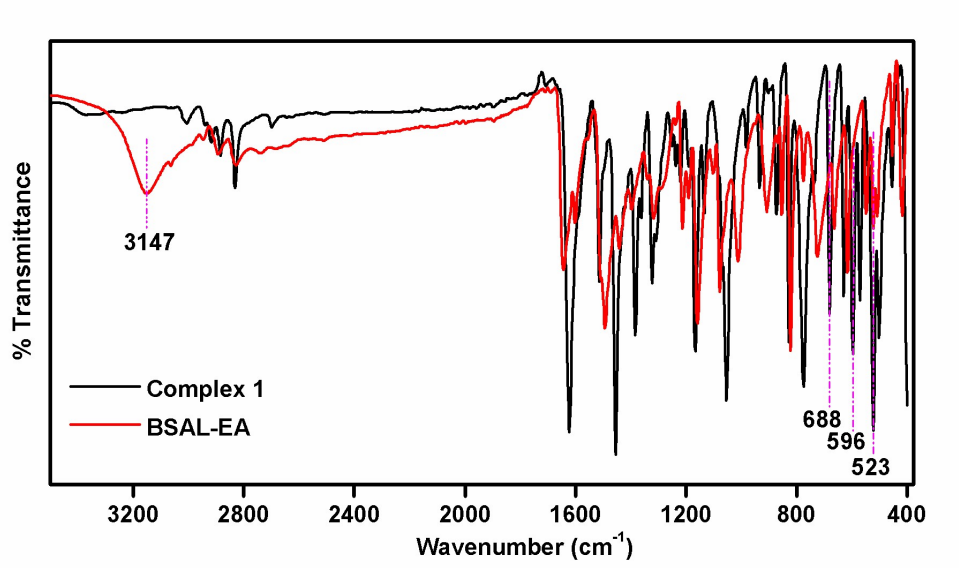

Fig. S5 FT-IR spectrum comparison of BSAL-EA and $[Me_2Sn(SAL\text{-}EA)]_2$

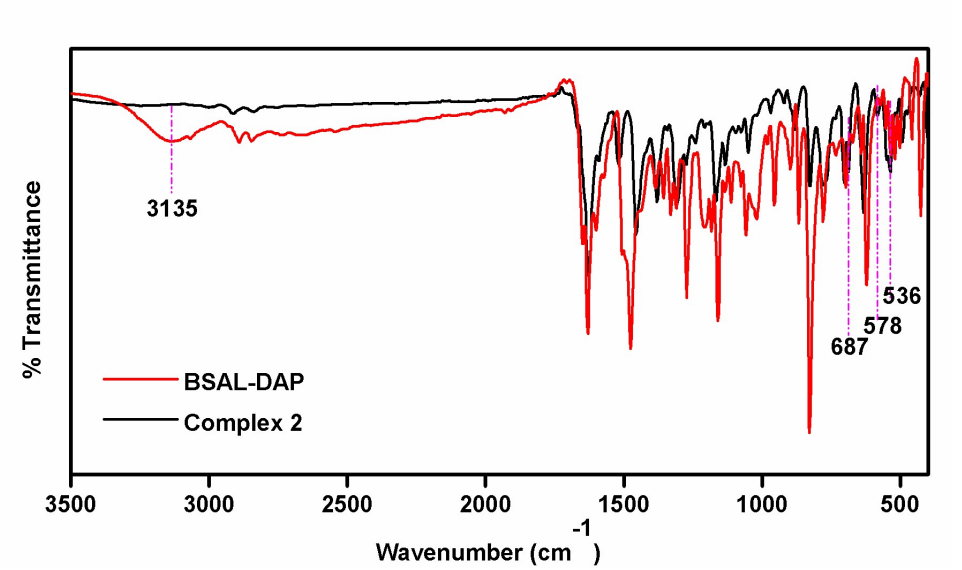

Fig. S6 FT-IR spectrum comparison of BSAL-DAP and $[Me_2Sn_2(BSAL\text{-}DAP)(BSAL)]$

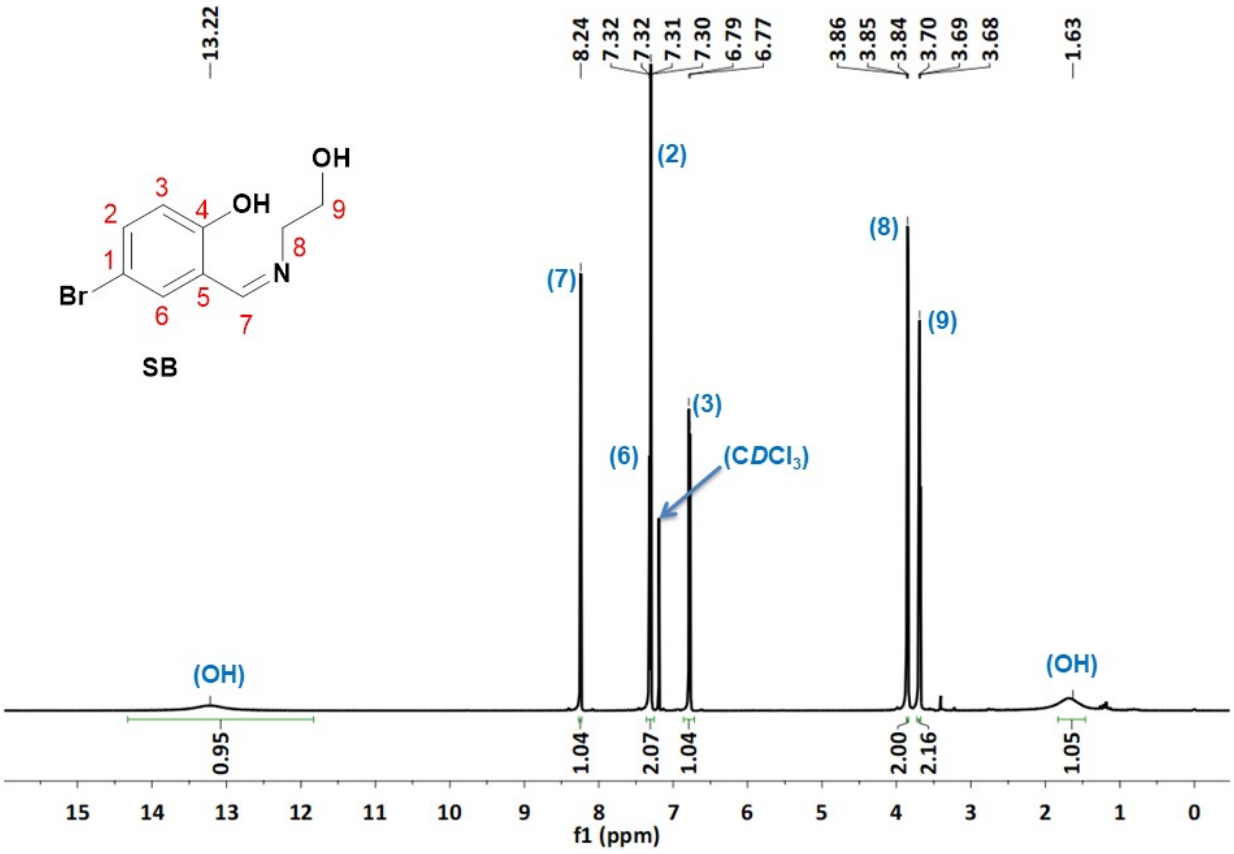

Figure S7 ^{1}H-NMR spectrum (500 MHz, $CDCl_3$) BSAL-EA.

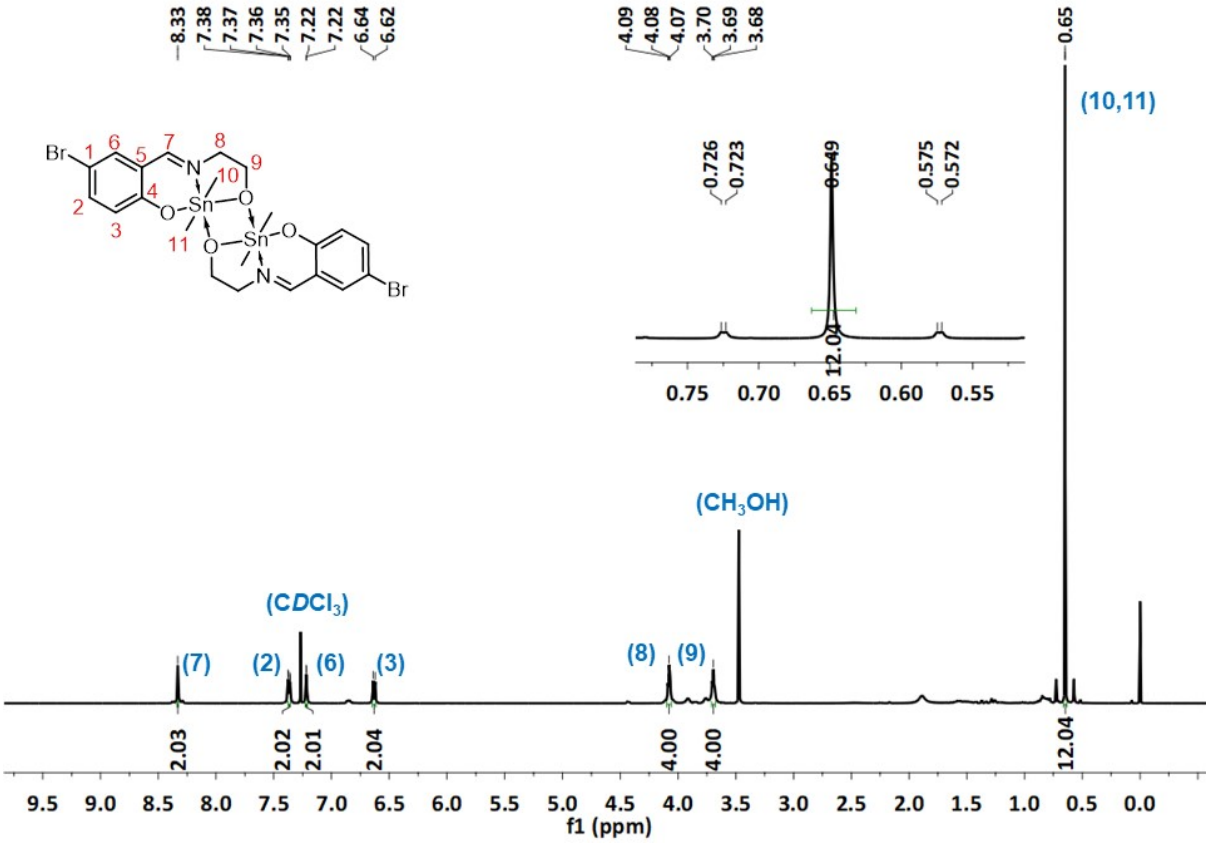

Fig. S8 ^{1}H-NMR spectrum (500 MHz, C*D*Cl$_3$) of [Me$_2$Sn(SAL-EA)]$_2$

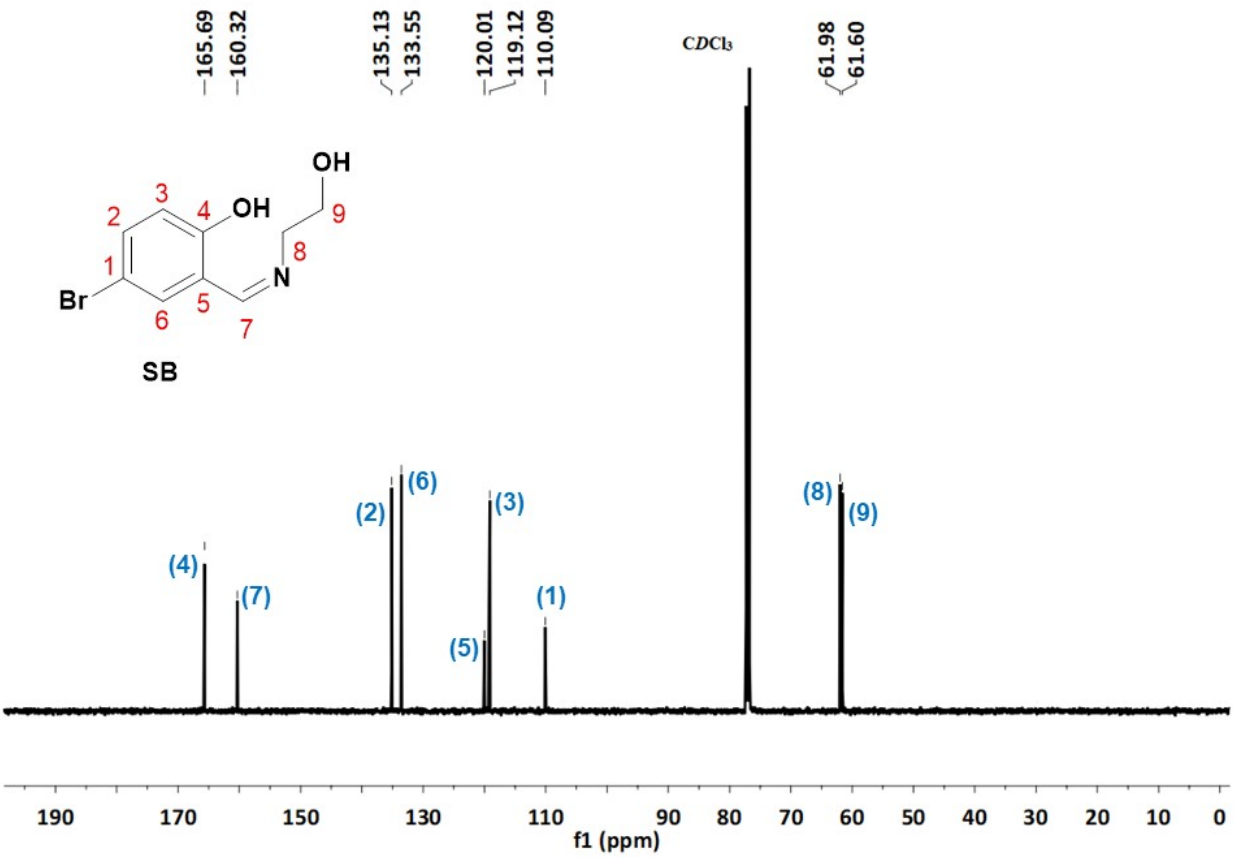

Figure S9 ^{13}C-NMR spectrum (125 MHz, $CDCl_3$) BSAL-EA.

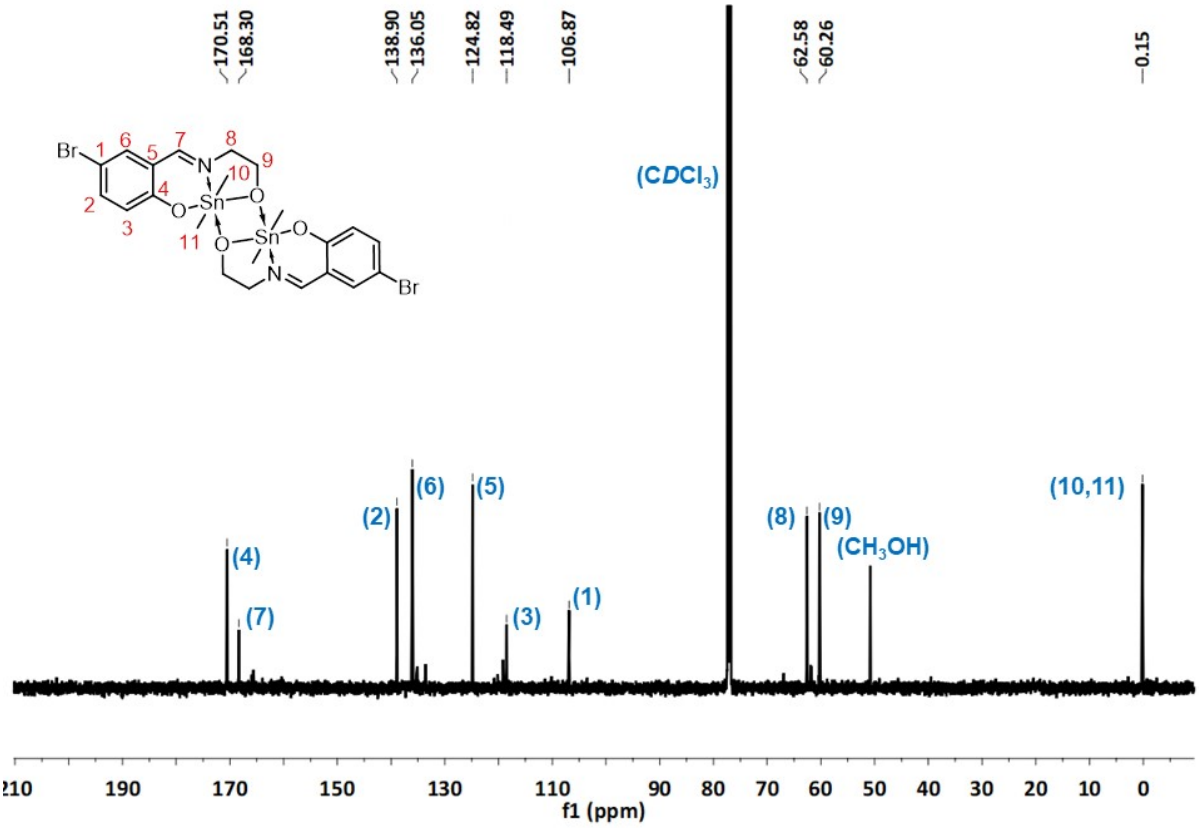

Fig. S10 ^{13}C NMR spectrum (125 MHz, C*D*Cl$_3$) of [Me$_2$Sn(SAL-EA)]$_2$

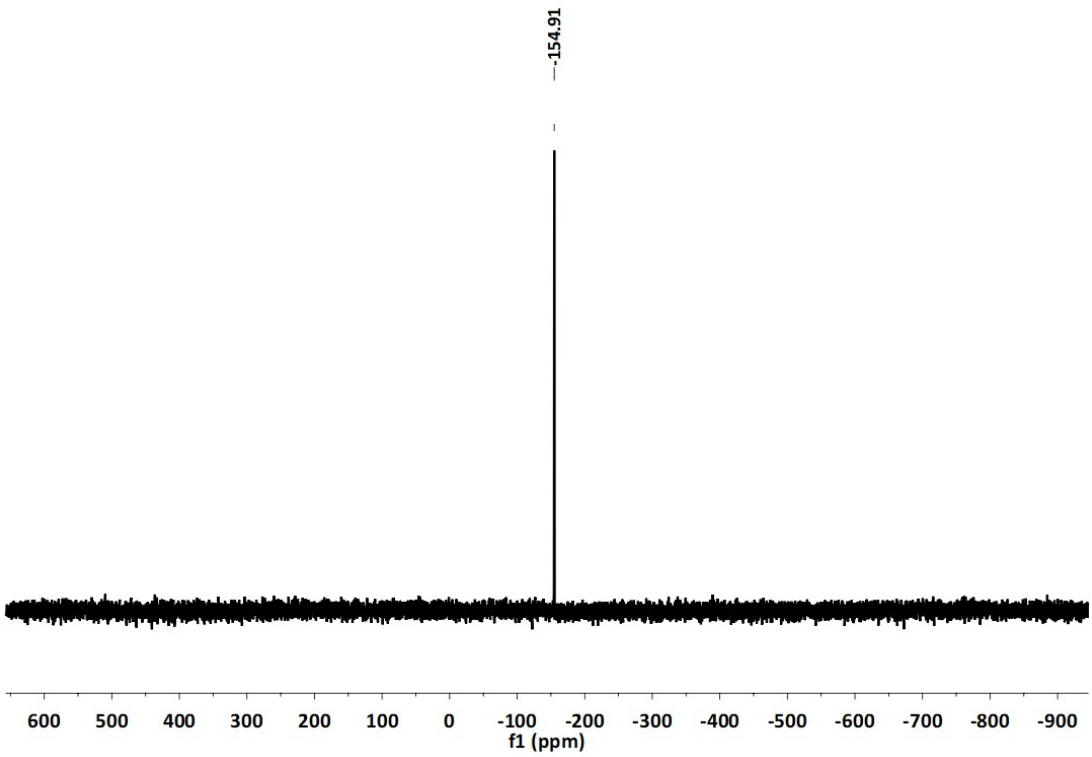

Fig. S11 ^{119}Sn NMR spectrum (186 MHz, C*D*Cl$_3$) of [Me$_2$Sn(SAL-EA)]$_2$

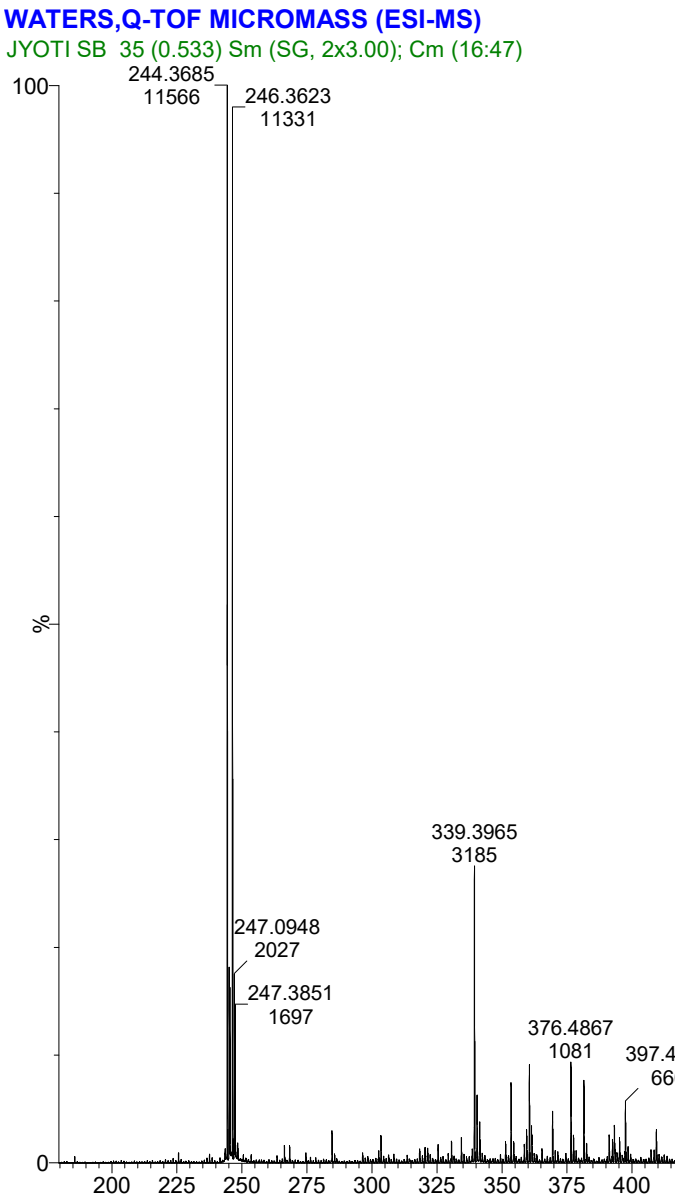

Figure S12 ESI-MS spectrum of Schiff base BSAL-EA.

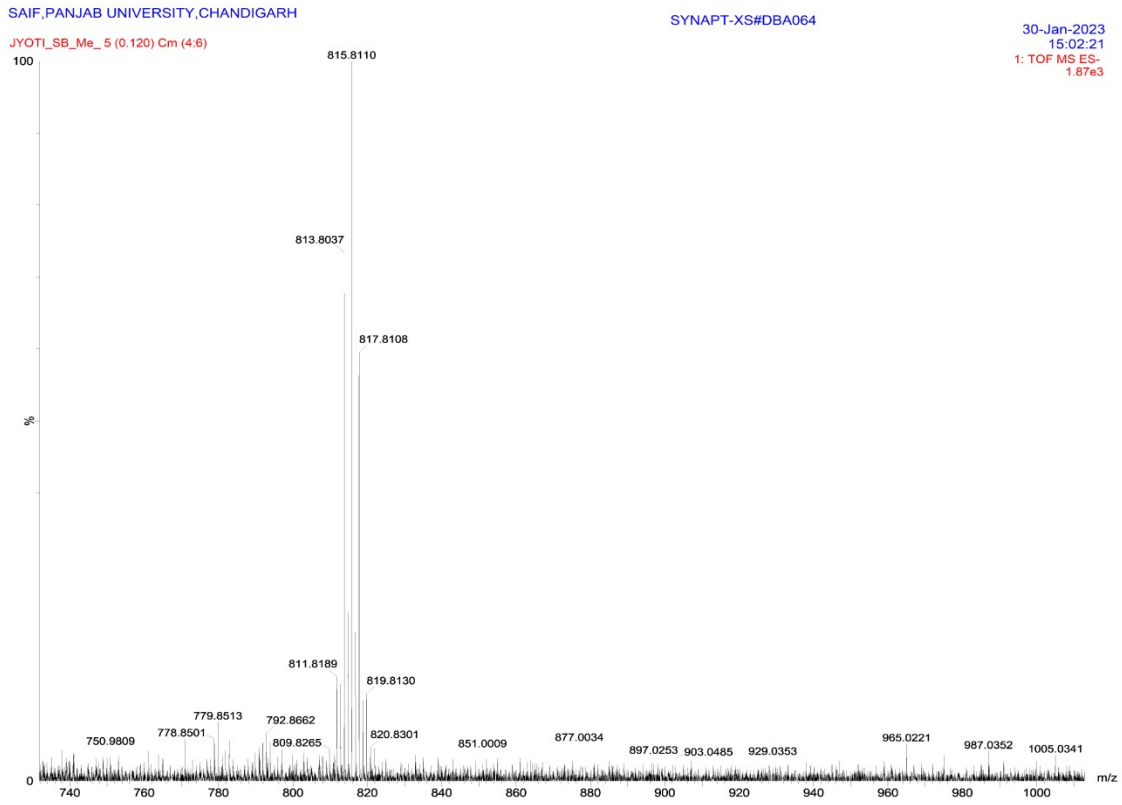

Fig. S13 ESI-MS spectrum of $[Me_2Sn(SAL\text{-}EA)]_2$

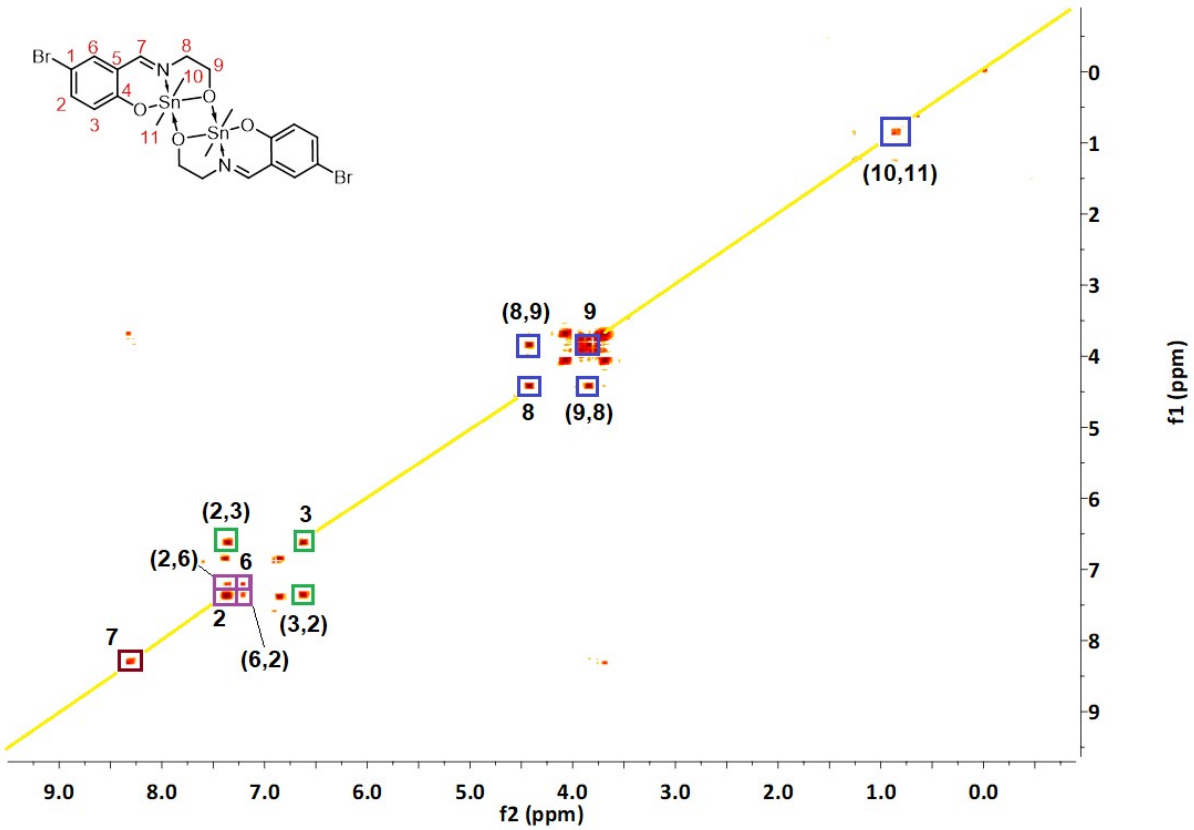

Fig. S14 (^{1}H-^{1}H) COSY NMR of Sn compound 1.

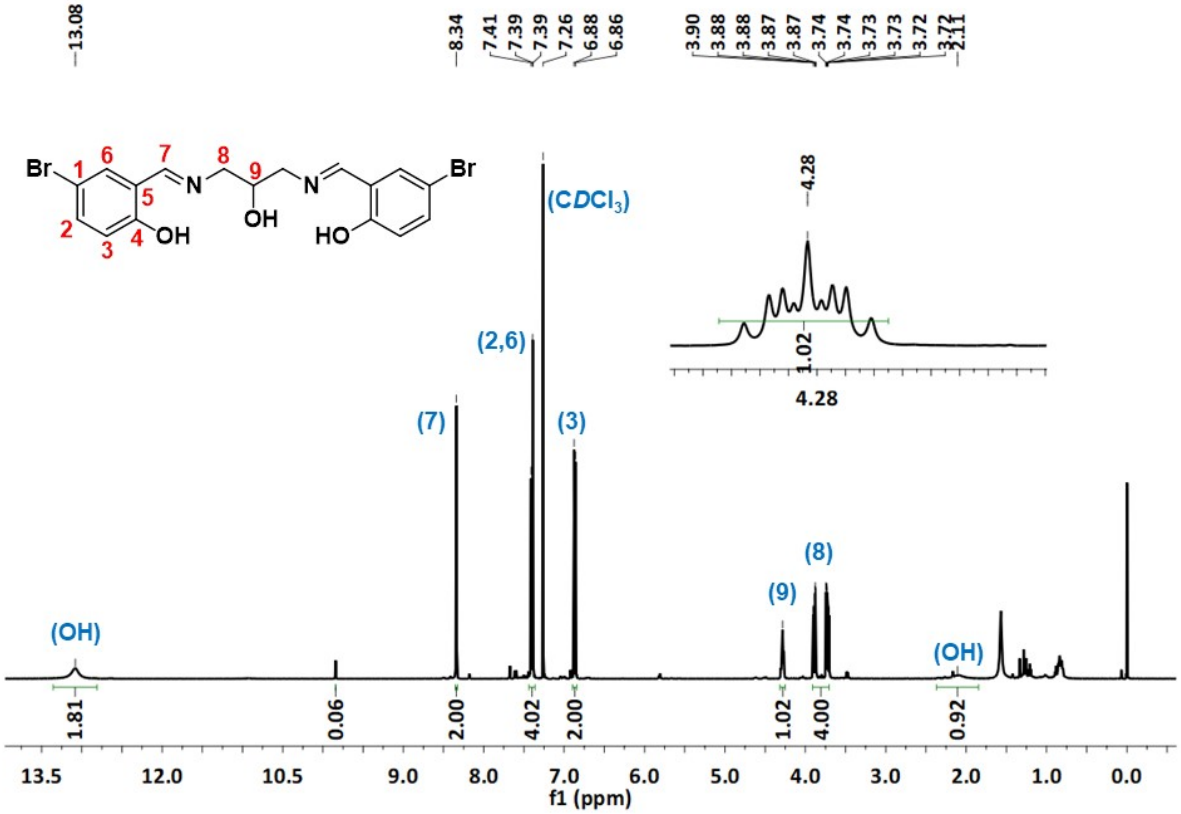

Fig. S15 ^{1}H-NMR spectrum (500 MHz, C*D*Cl$_3$) of BSAL-DAP

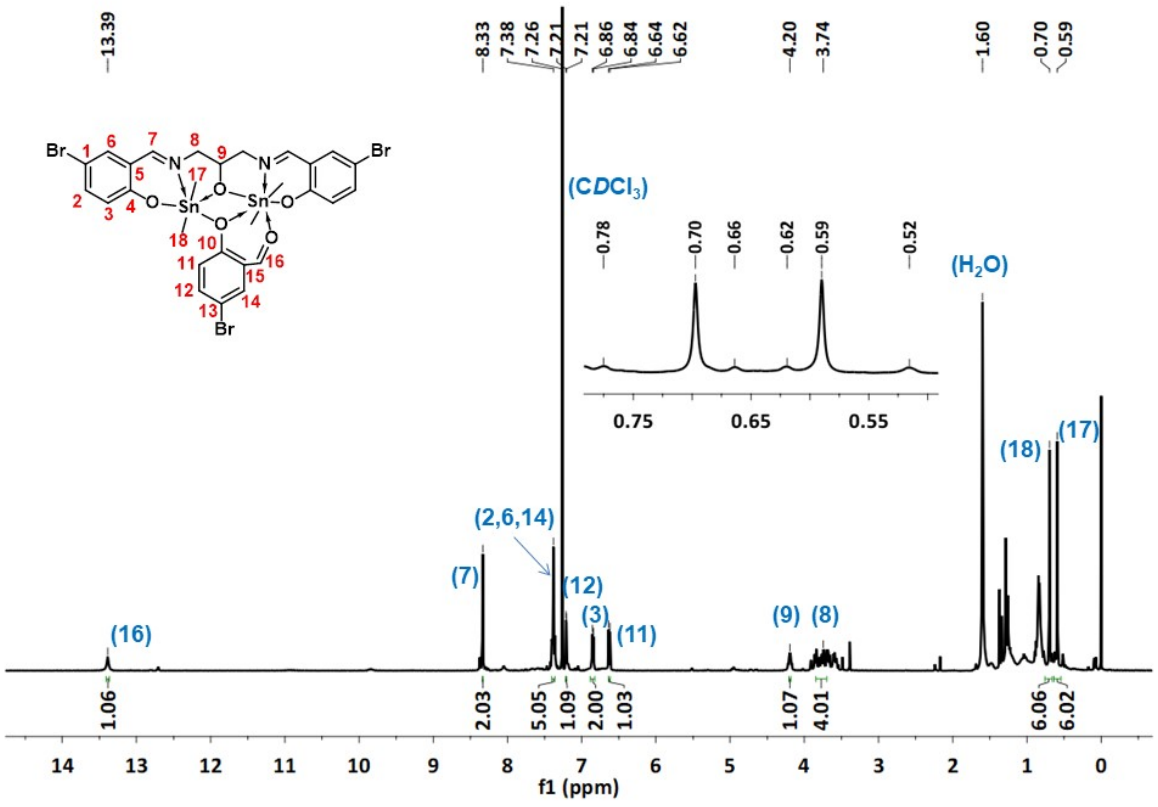

Fig. S16 ^{1}H-NMR spectrum (500 MHz, C*D*Cl$_3$) of [Me$_2$Sn$_2$(BSAL-DAP)(BSAL)]

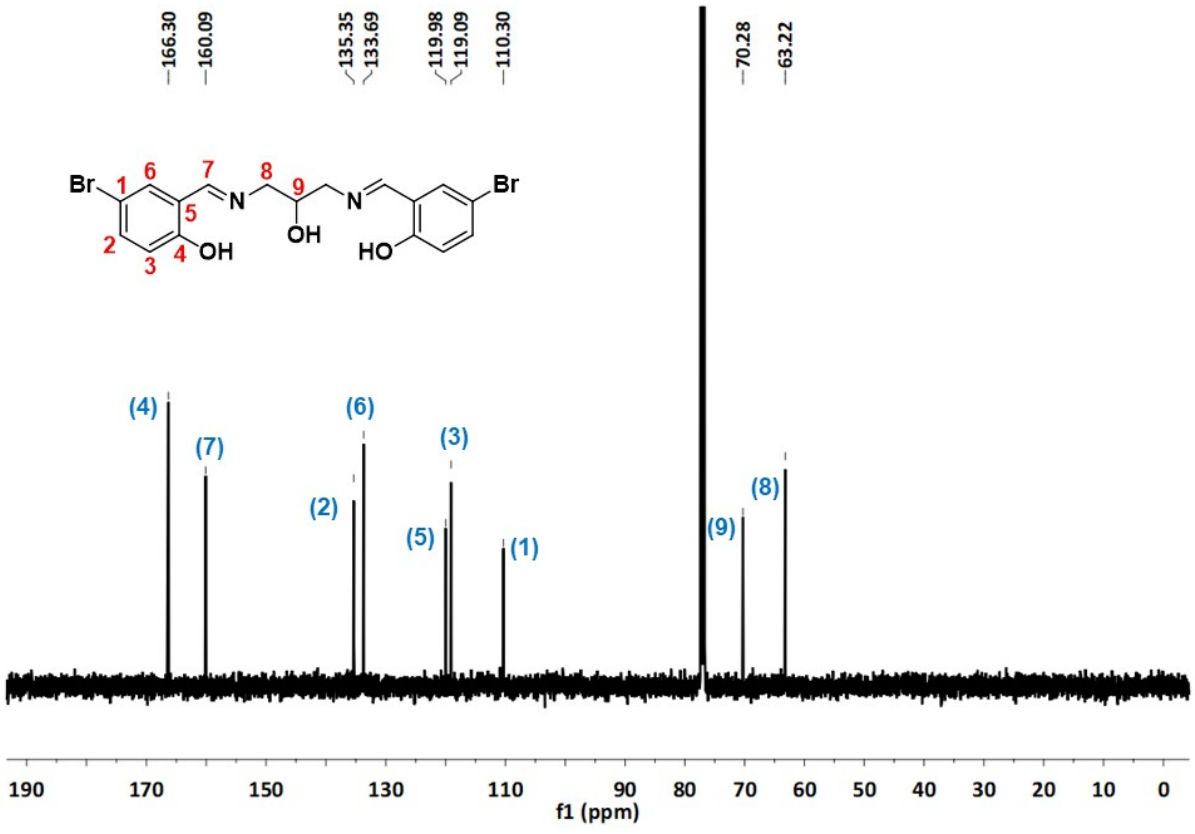

Fig. S17 ^{13}C NMR spectrum (125 MHz, C*D*Cl$_3$) of BSAL-DAP

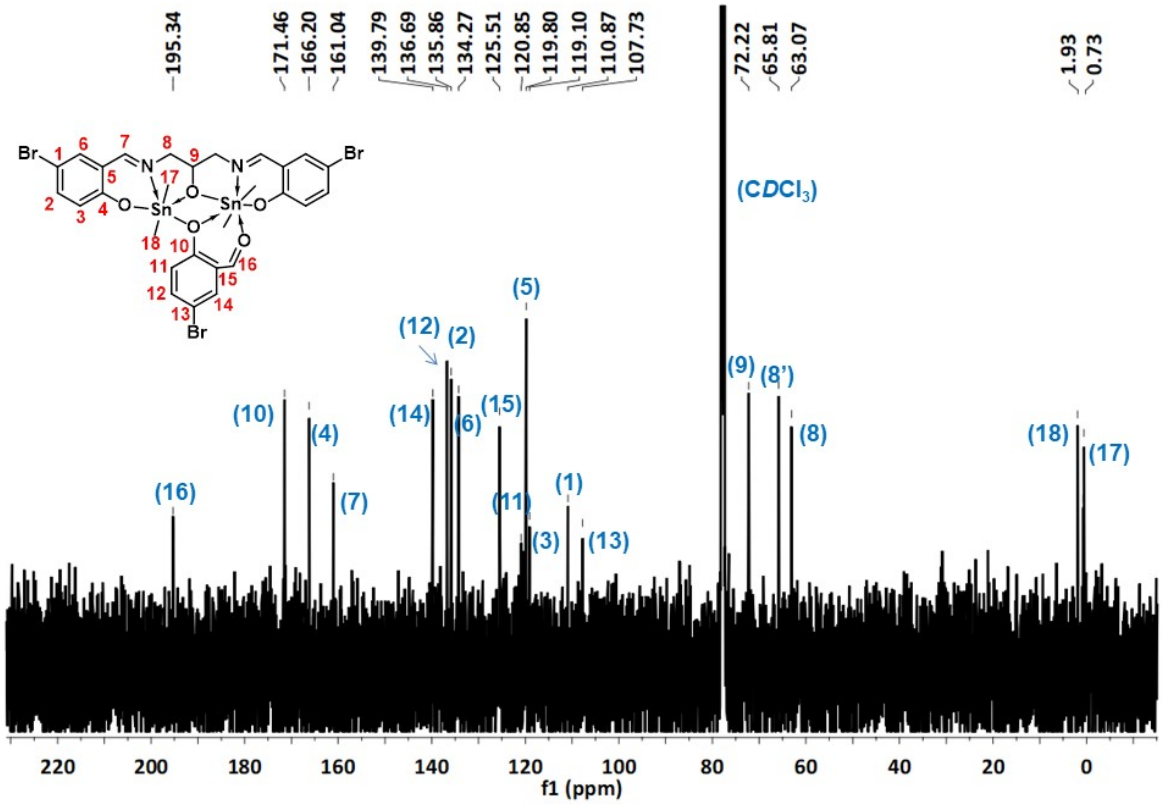

Fig. S18 ^{13}C NMR spectrum (125 MHz, C*D*Cl$_3$) of [Me$_2$Sn$_2$(BSAL-DAP)(BSAL)]

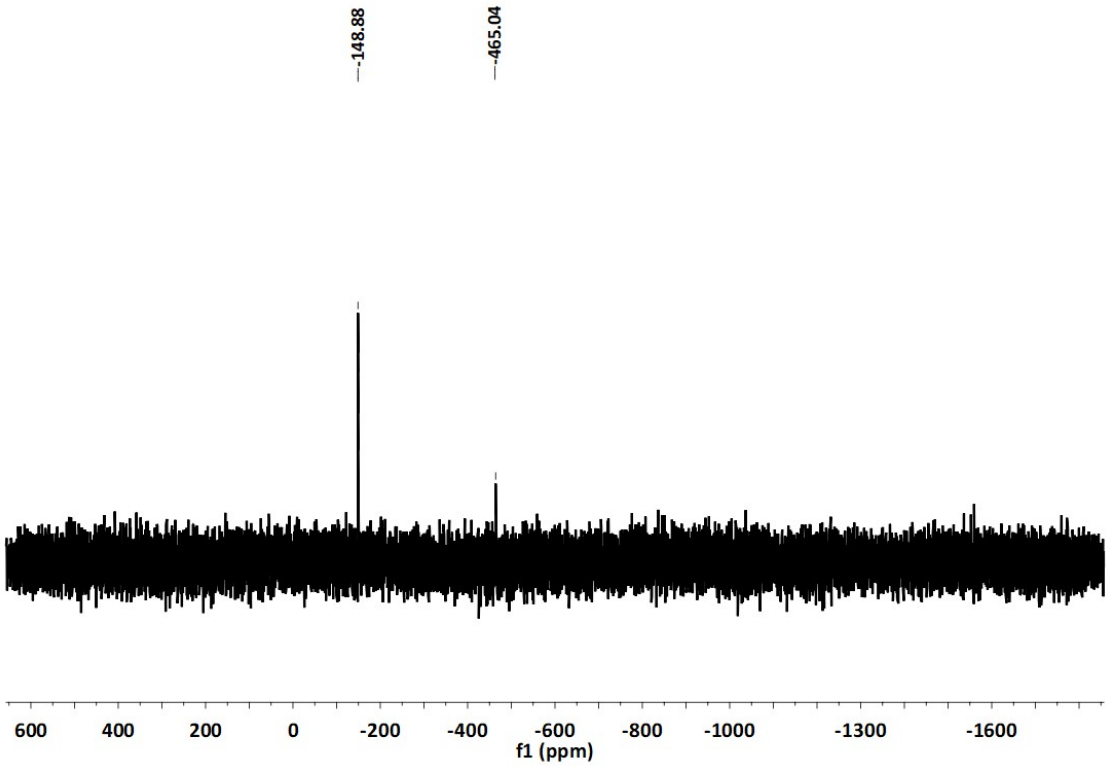

Fig. S19 ^{119}Sn NMR spectrum (186 MHz, C*D*Cl$_3$) of [Me$_2$Sn$_2$(BSAL-DAP)(BSAL)]

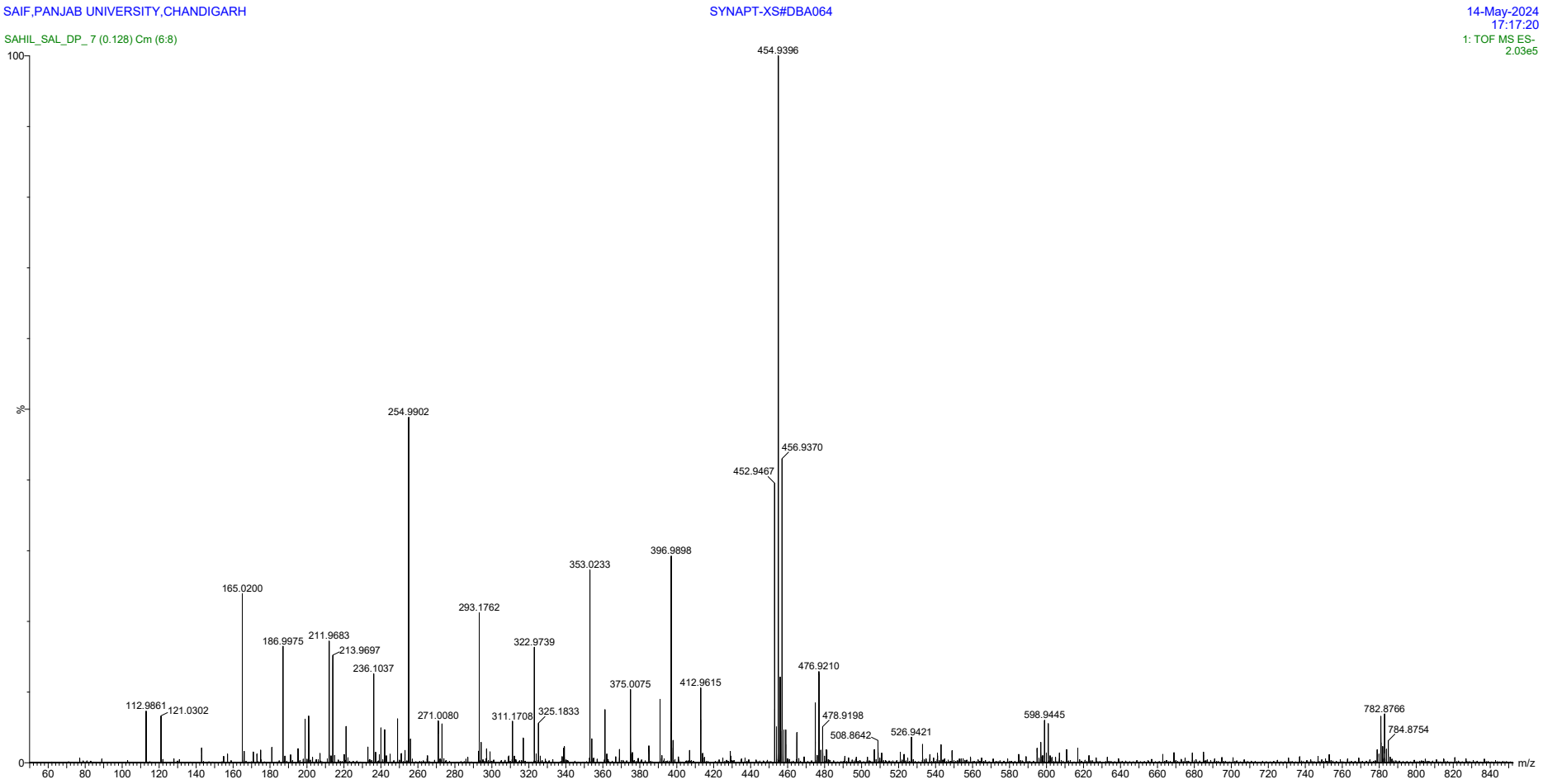

Fig. S20 ESI-MS spectrum of BSAL-DAP

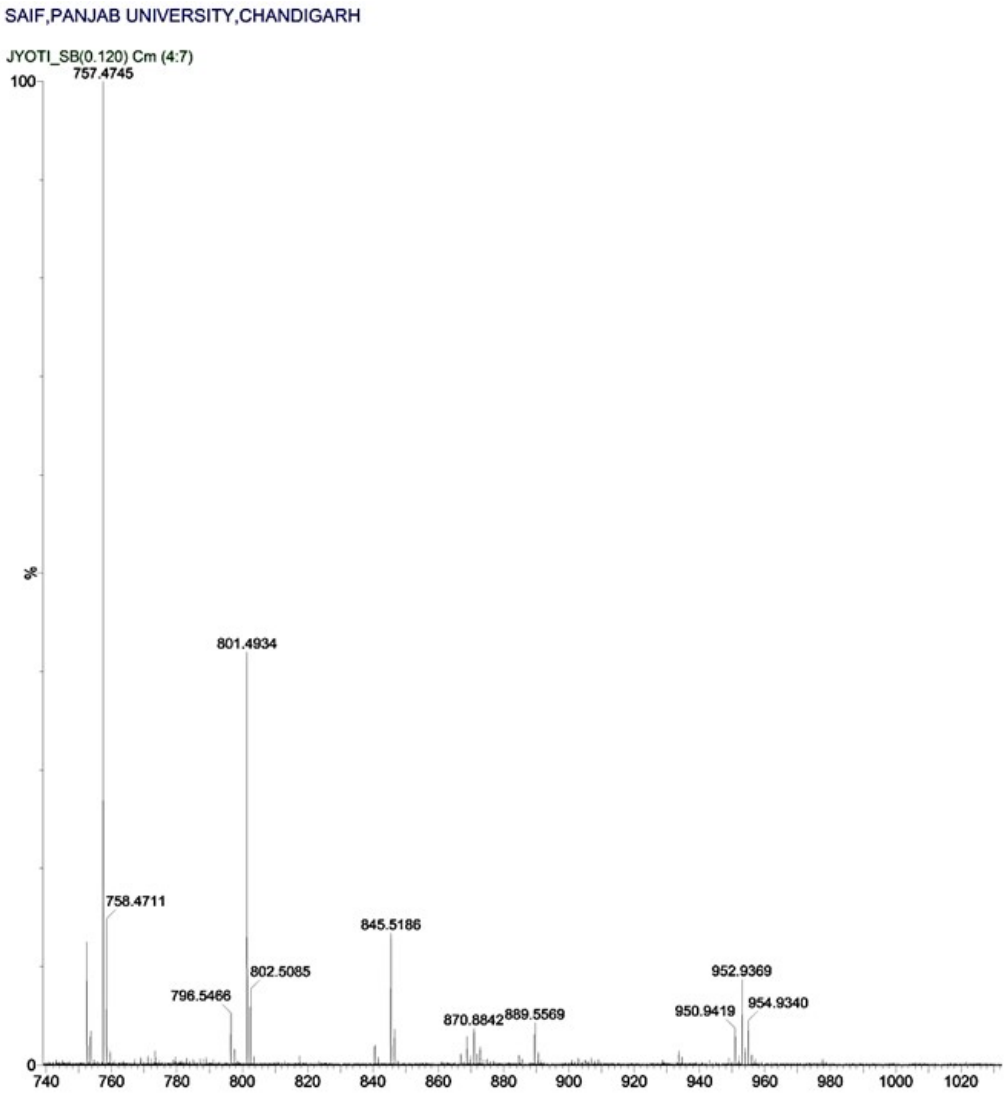

Fig. S21 ESI-MS spectrum of [Me_2Sn_2(BSAL-DAP)(BSAL)]

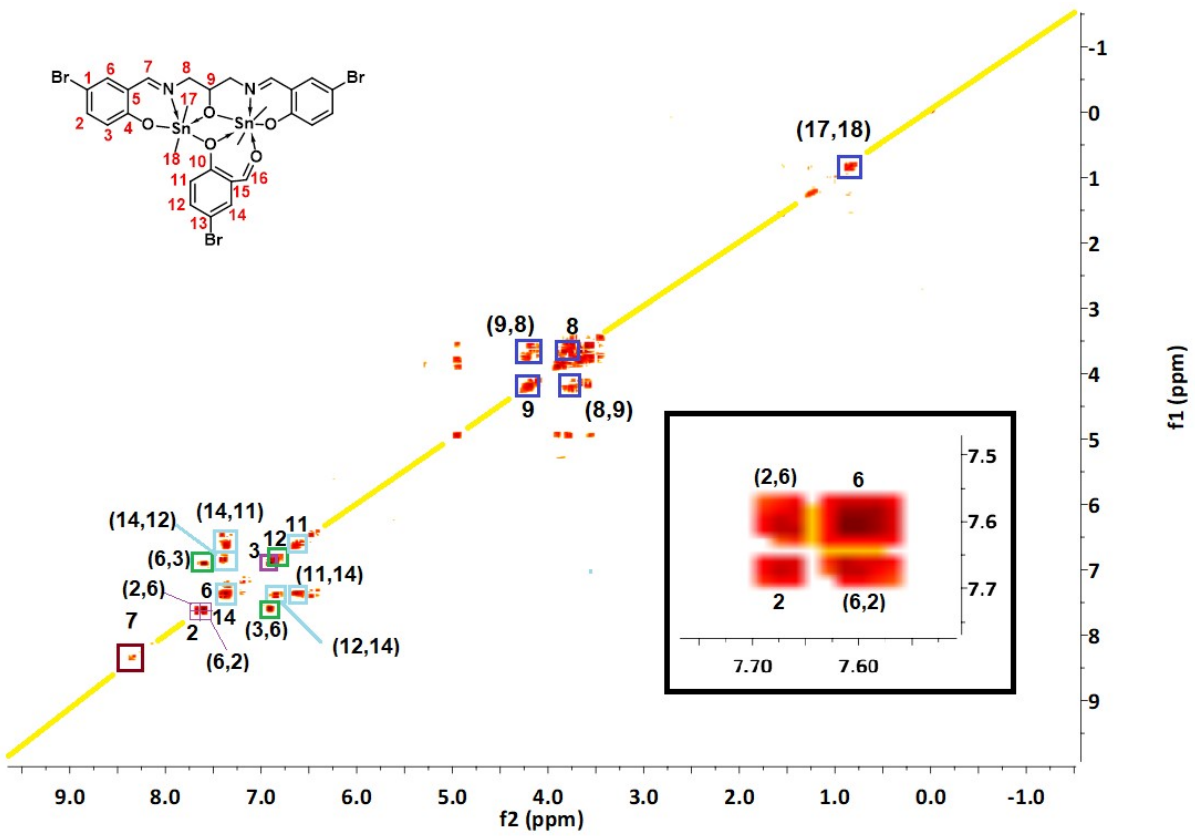

Fig. S22 (^{1}H-^{1}H) COSY NMR of Sn compound 2.

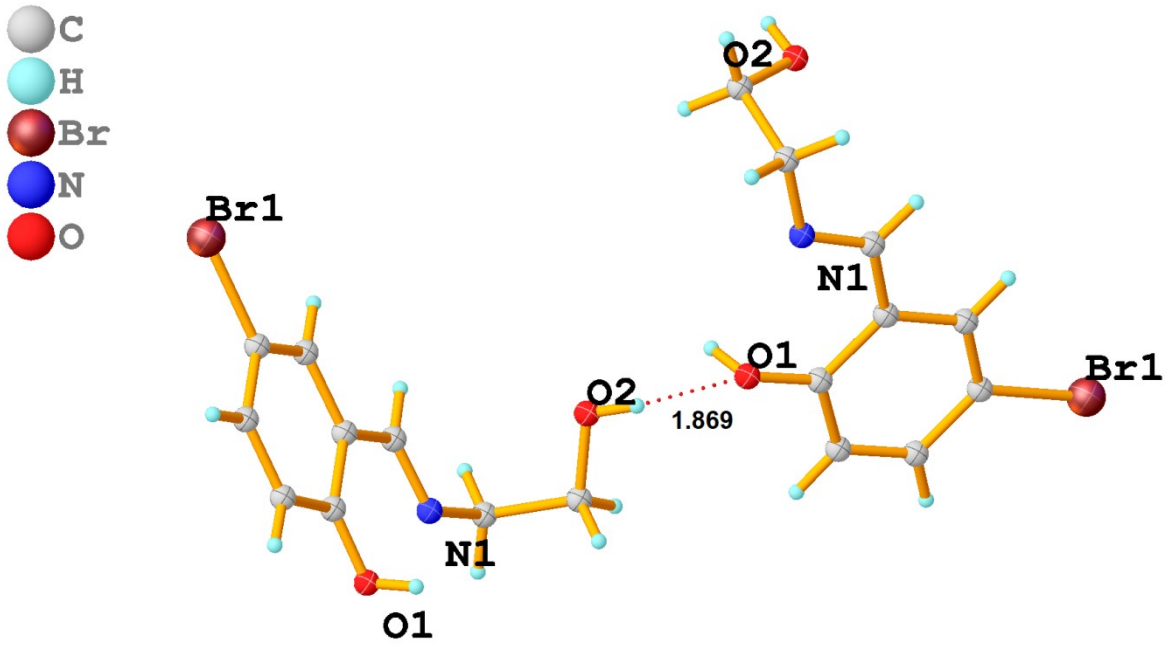

Fig. S23 ORTEP representation of BSAL-EA showing intermolecular hydrogen bonding,

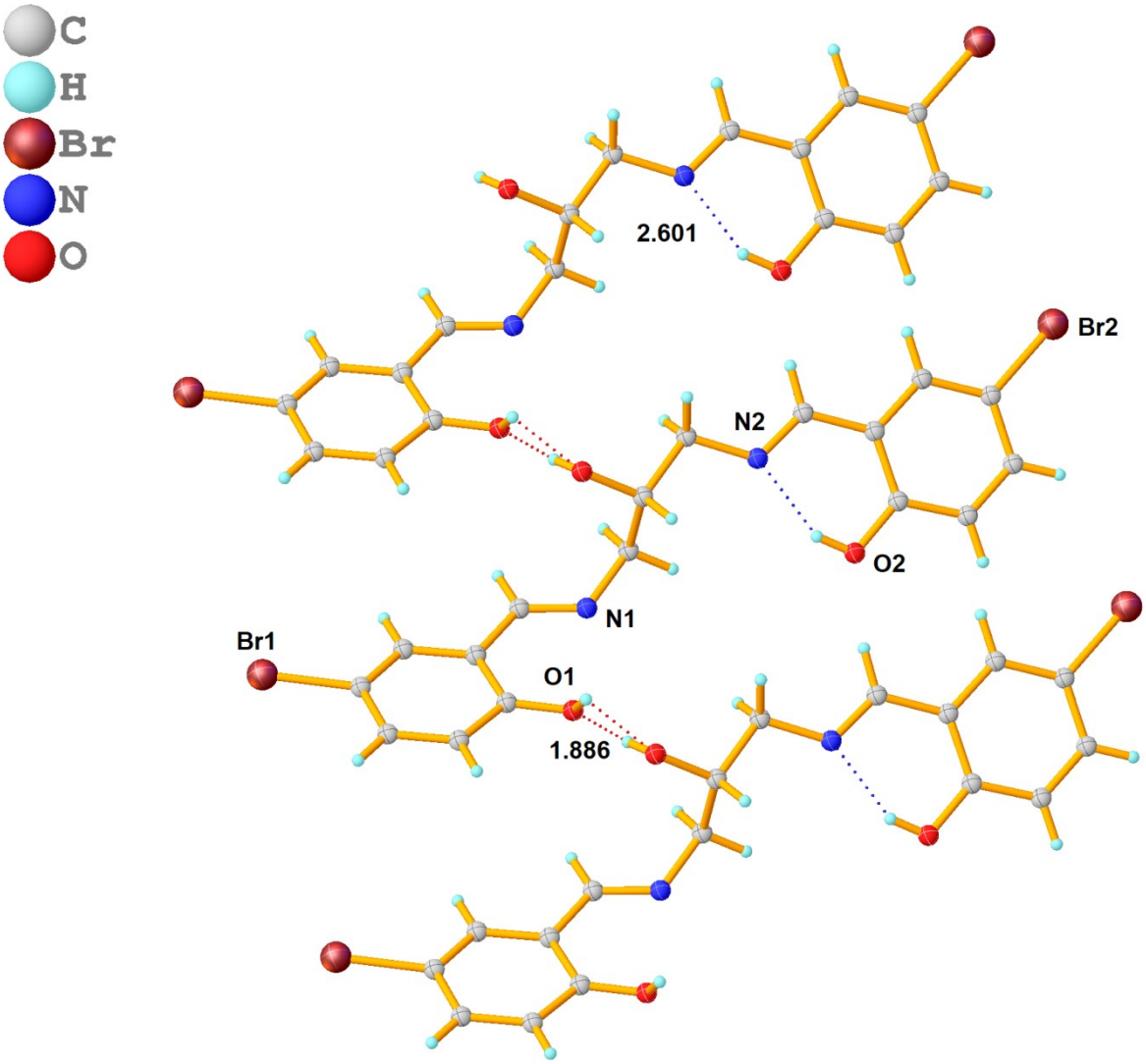

Fig. S24 ORTEP representation of BSAL-DAP showing inter-/intra-molecular hydrogen bonding,

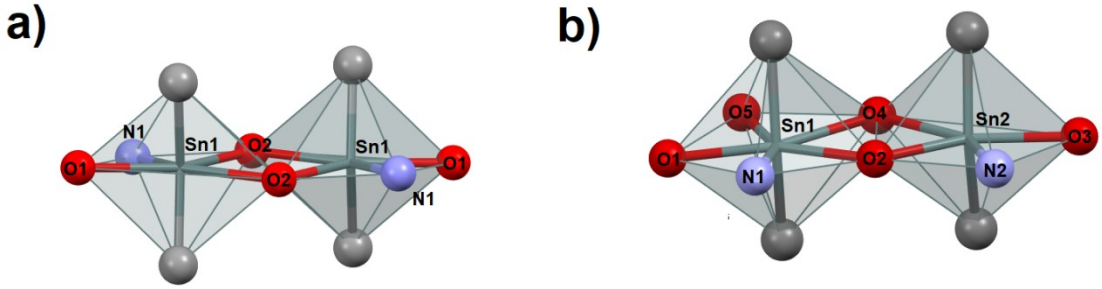

Fig. S25 a) topographical view of coordination in Compound 1, and **b)** topographical view of coordination in Compound 2 (for non-hydrogen atoms, the radius of hydrogen atoms was eliminated for clarity).

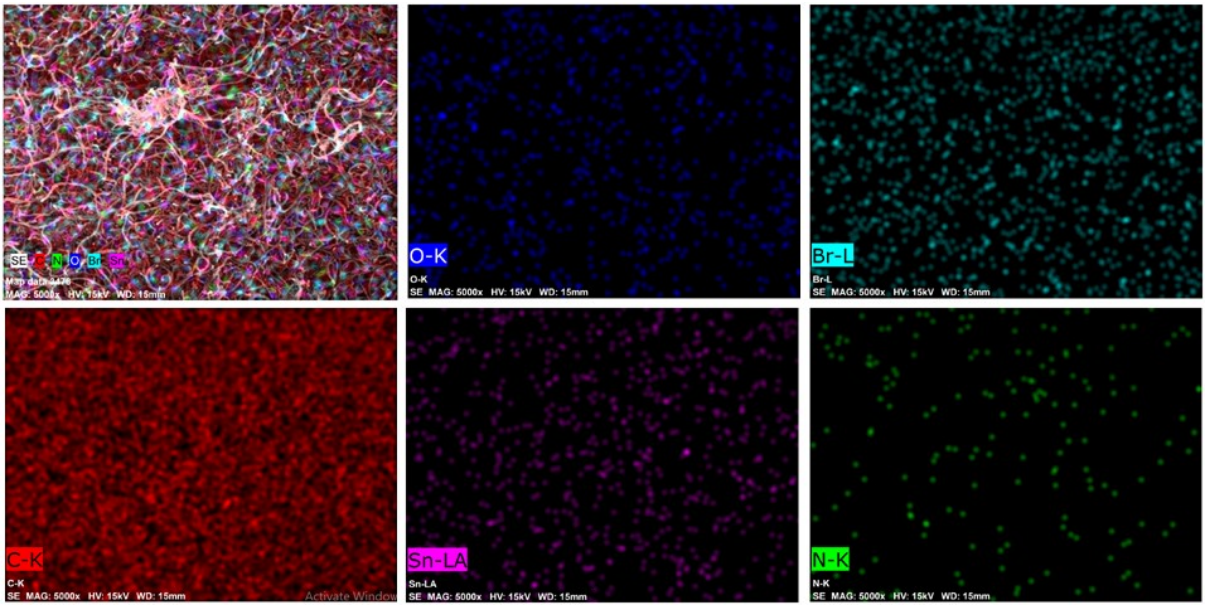

Fig. S26 Elemental mapping of all elements of the 1@CNT (C, O, N, Br, and Sn) at the surface.

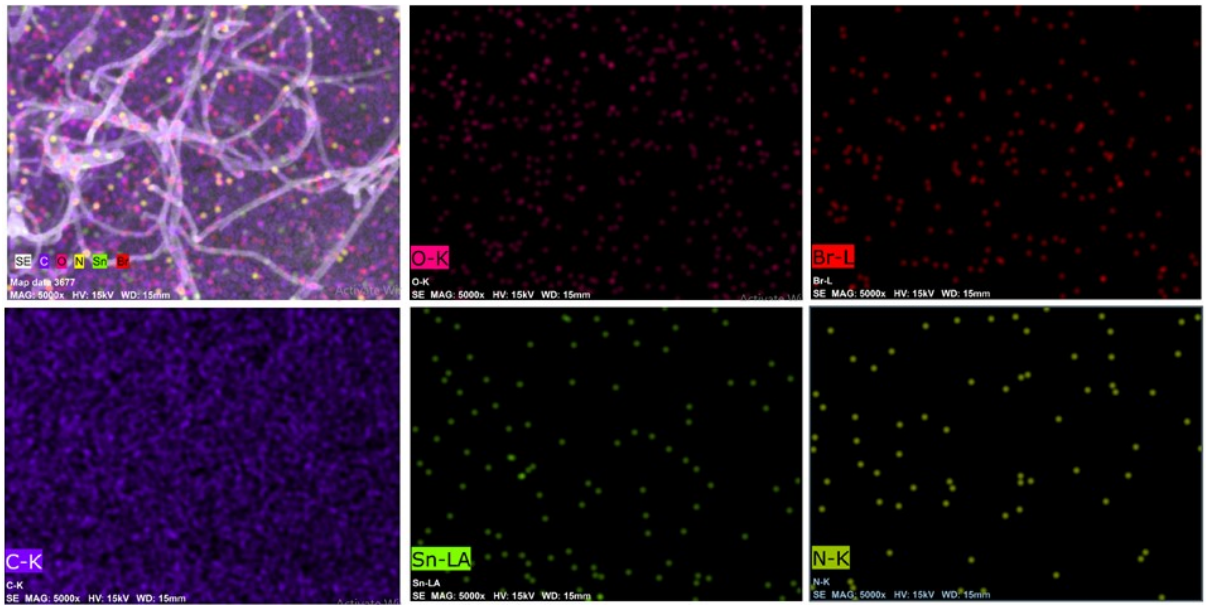

Fig. S27 Elemental mapping of all elements of the 2@CNT (C, O, N, Br, and Sn) at the surface.

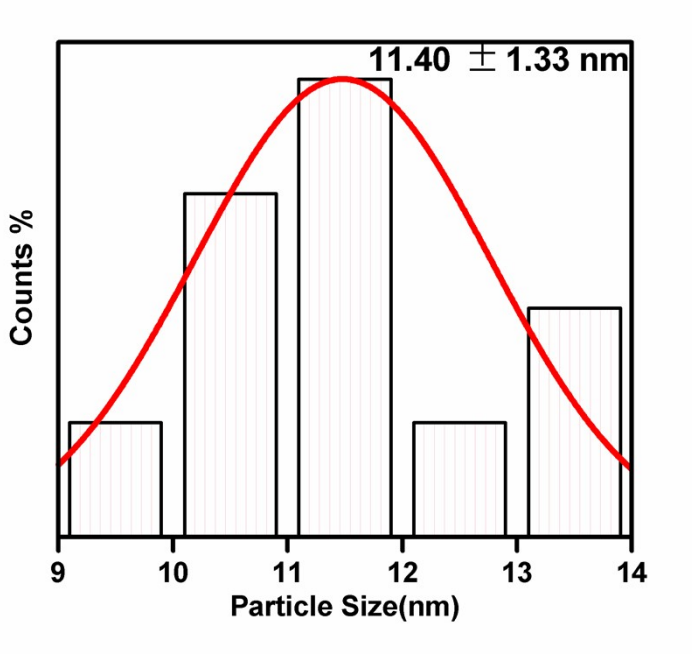

Fig. S28 Particle size distribution of 2@CNT

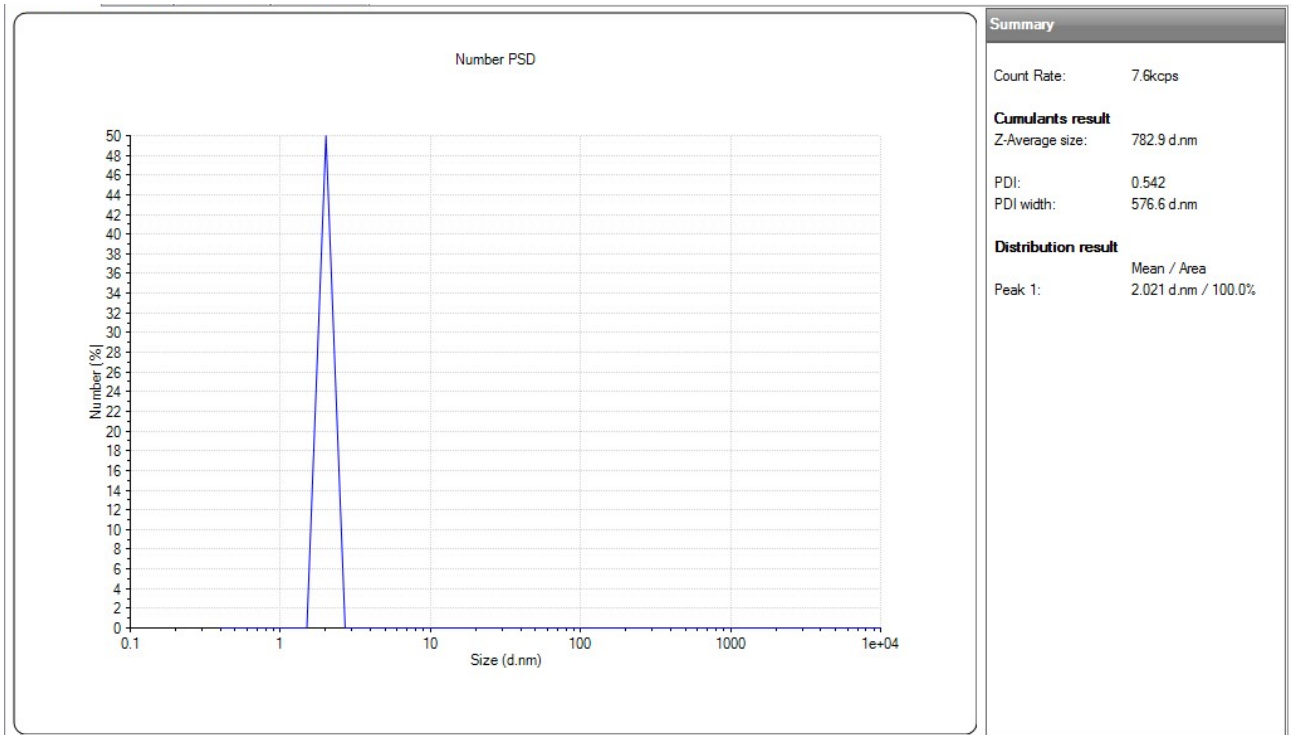

Fig. S29 DLS particle size distribution of compound 1

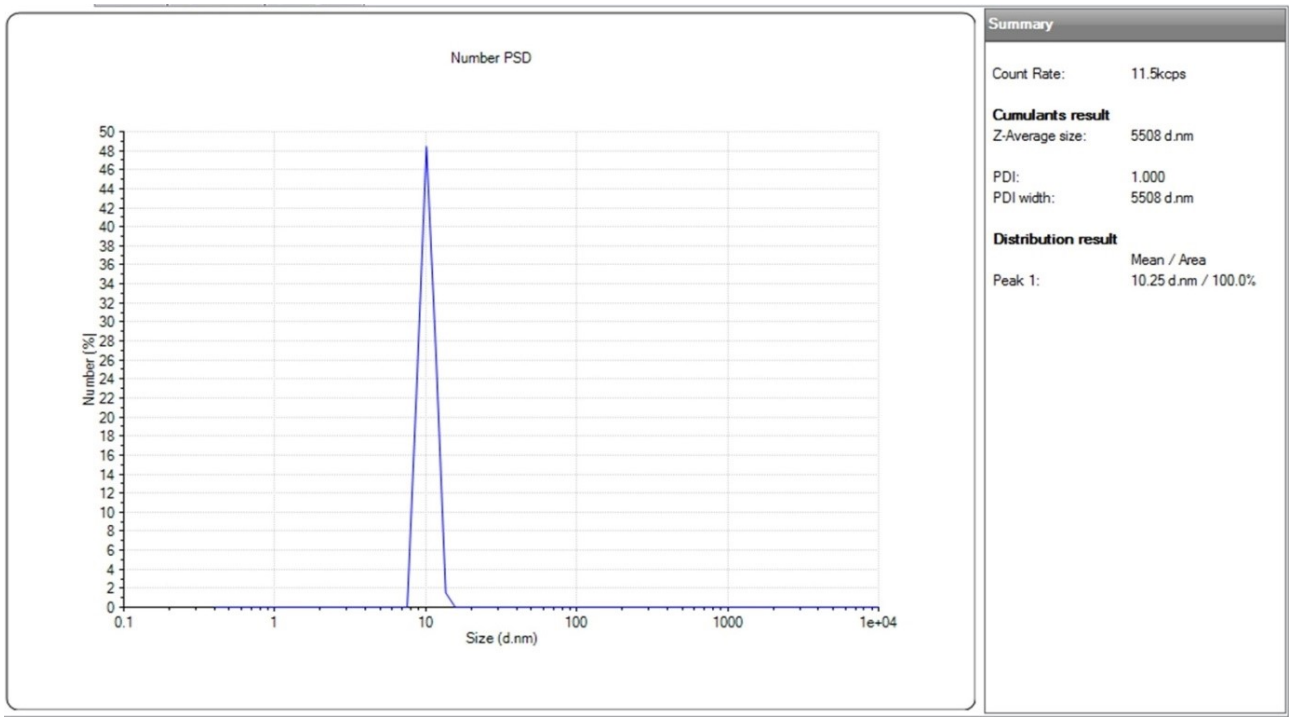

Fig. S30 DLS particle size distribution of compound 2

			Size (d.nm):	% Volume:	St Dev (d.nm):
Z-Average (d.nm):	805.2	Peak 1:	207.9	100.0	28.10
PdI:	0.956	Peak 2:	0.000	0.0	0.000
Intercept:	0.962	Peak 3:	0.000	0.0	0.000

Result quality : Refer to quality report

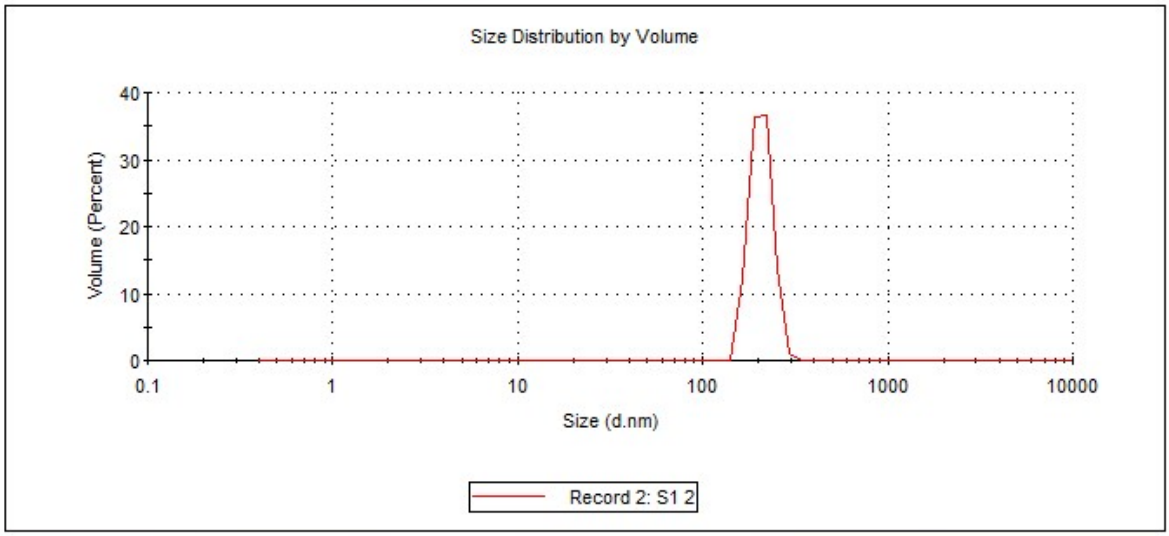

Fig. S31 DLS particle size distribution of 1@CNT

			Size (d.nm):	% Volume:	St Dev (d.nm):
Z-Average (d.nm):	636.8	Peak 1:	566.1	100.0	77.55
PdI:	0.741	Peak 2:	0.000	0.0	0.000
Intercept:	0.823	Peak 3:	0.000	0.0	0.000

Result quality : Refer to quality report

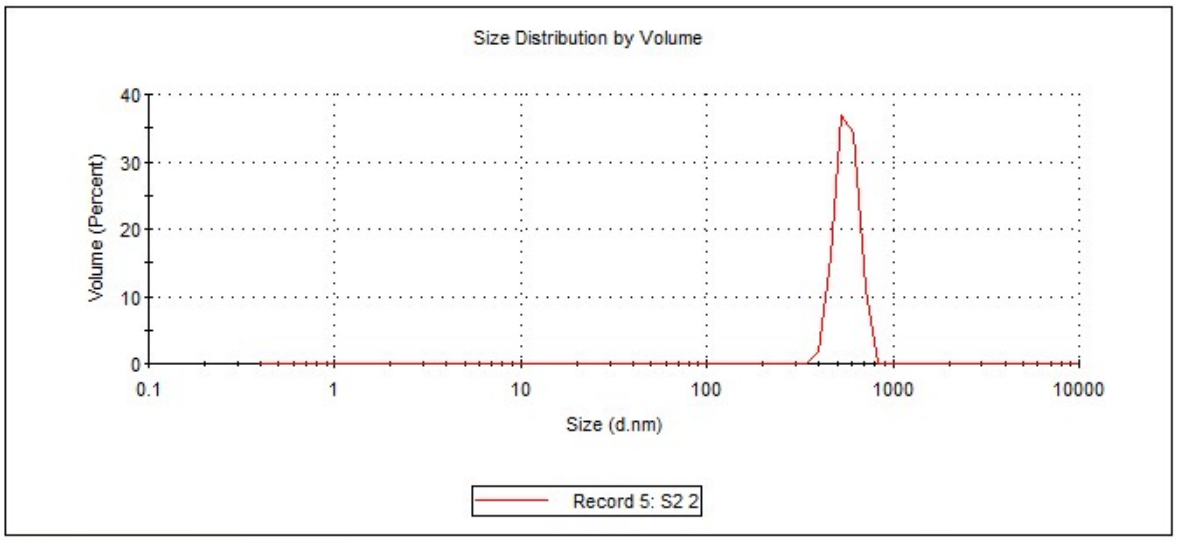

Fig. S32 DLS particle size distribution of 2@CNT

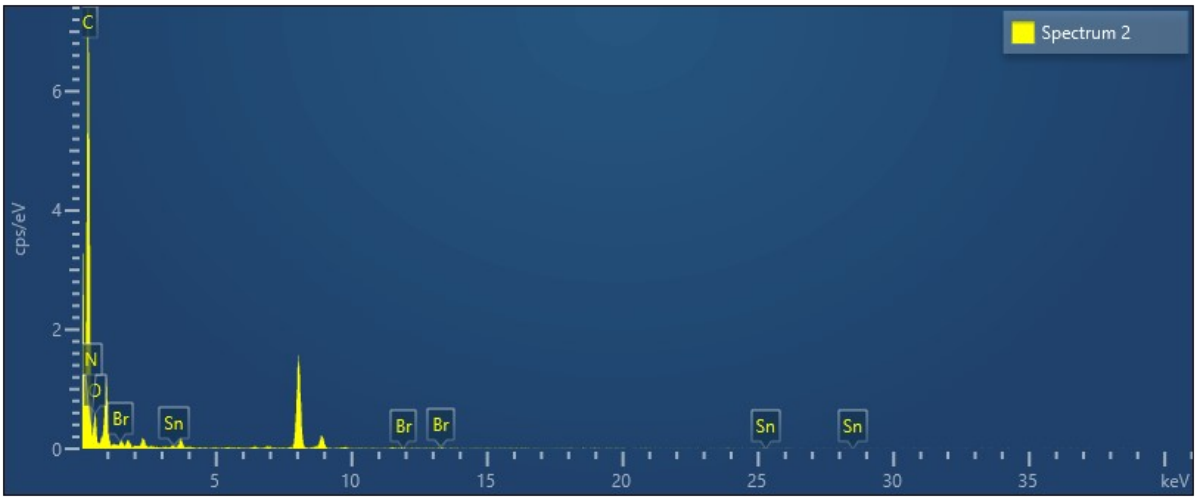

Fig. S33 EDAX distribution of 1@CNT

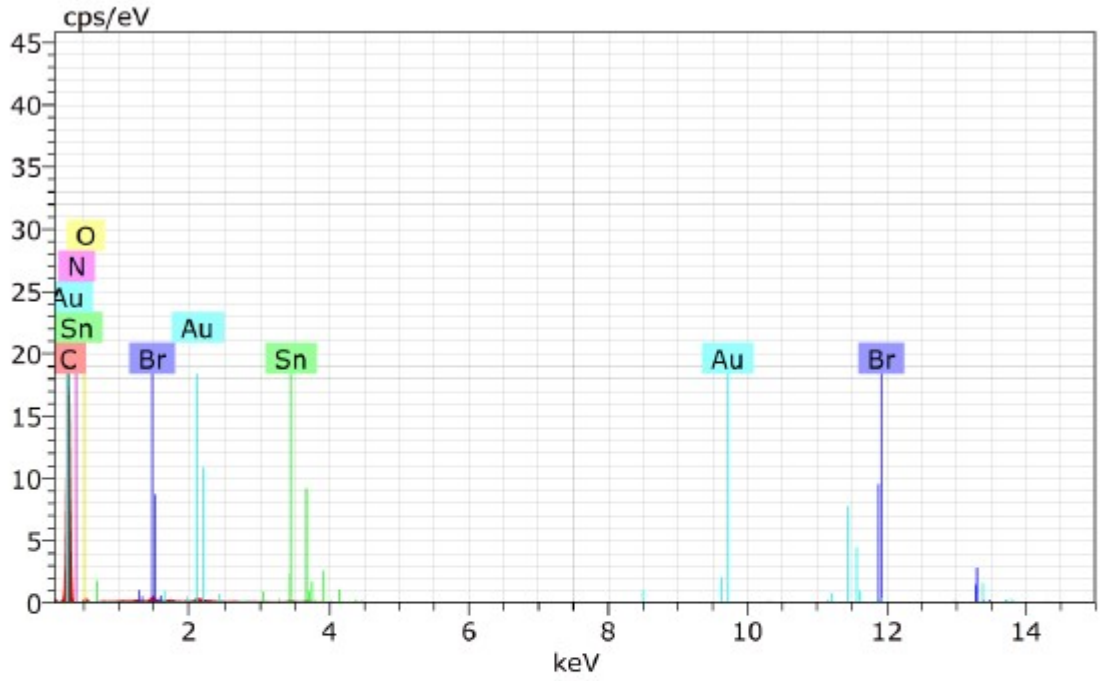

Spectrum: test 17394

Element	Series	unn. C [wt.%]	norm. C [wt.%]	Atom. C [at.%]	Error (3 Sigma) [wt.%]
Carbon	K-series	85.40	85.40	92.92	29.29
Tin	L-series	2.15	2.15	0.24	0.34
Bromine	L-series	2.06	2.06	0.34	0.41
Gold	M-series	2.92	2.92	0.19	0.46
Nitrogen	K-series	1.82	1.82	1.70	2.11
Oxygen	K-series	5.65	5.65	4.62	3.30
	Total:	100.00	100.00	100.00	

Fig. S34 EDAX distribution of 2@CNT

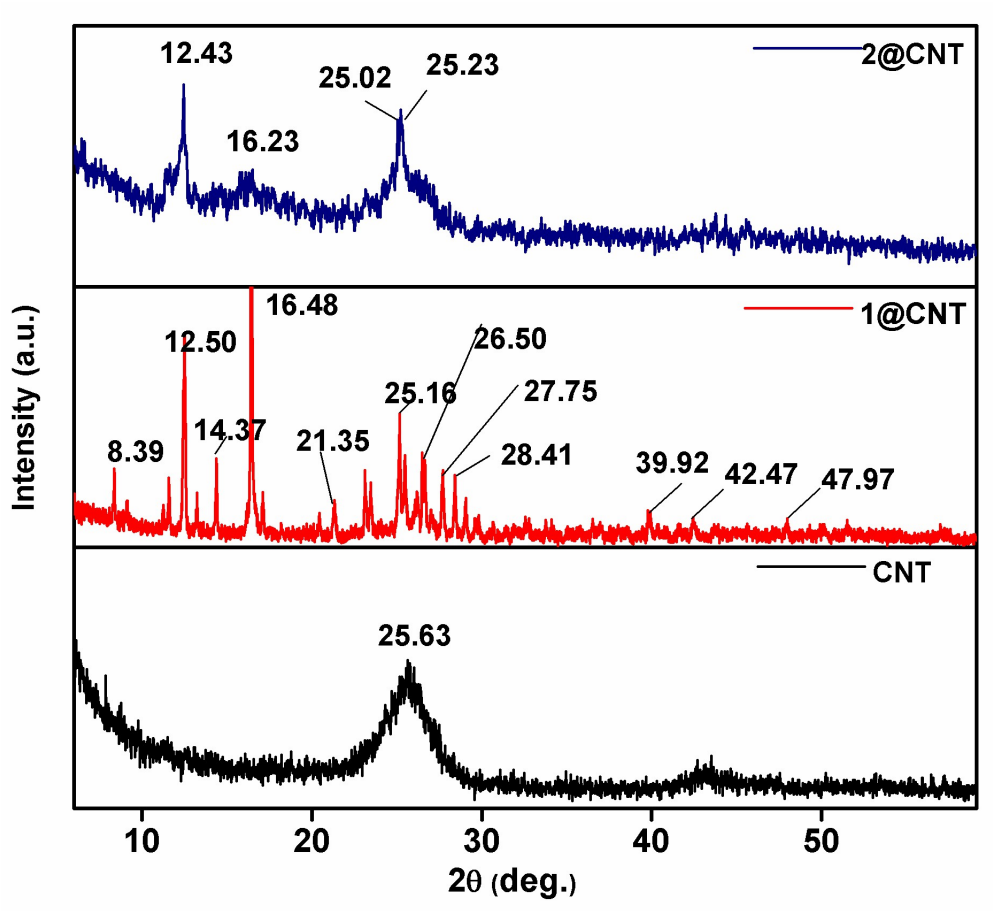

Fig. S35. PXRD pattern showing a comparison of data for **a)** CNT, **b)** 1@CNT, and **c)** 2@CNT.

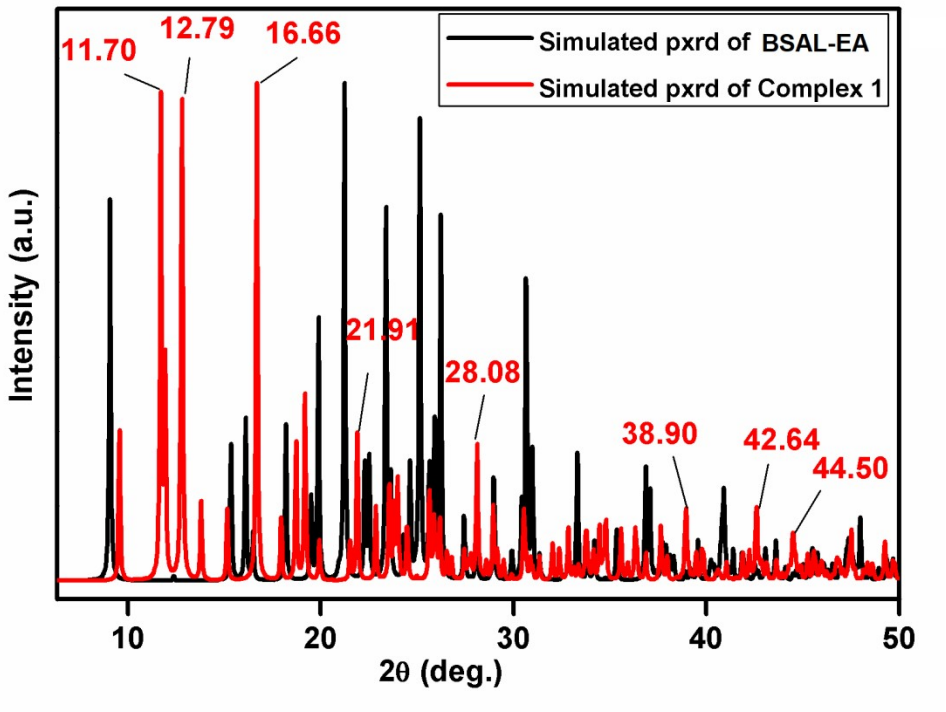

Fig. S36 Simulated PXRD pattern comparison of BSAL-EA and organotin Complex 1

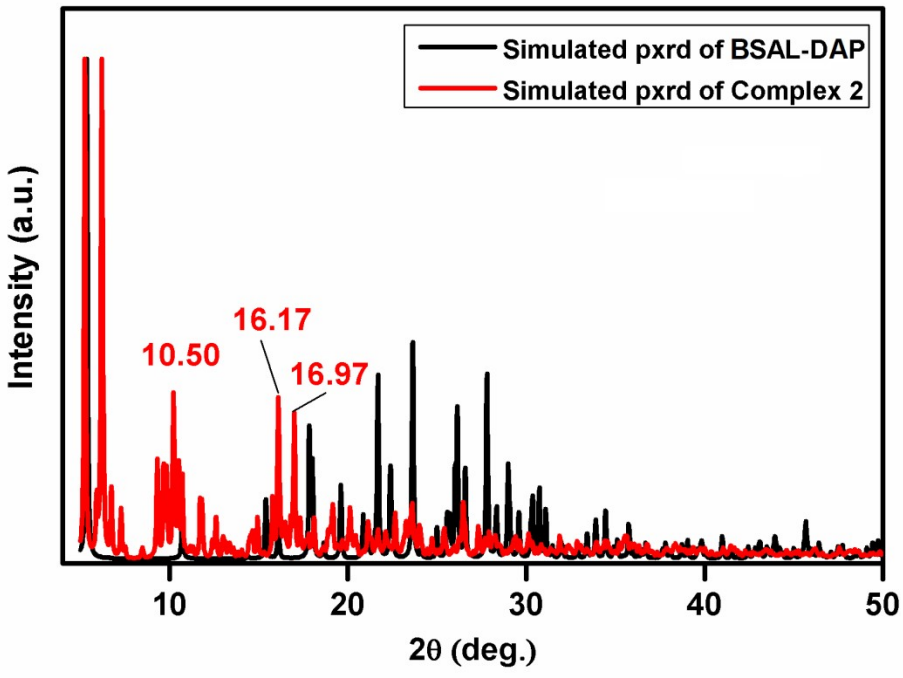

Fig. S37 Simulated PXRD pattern comparison of BSAL-DAP and organotin Complex 2

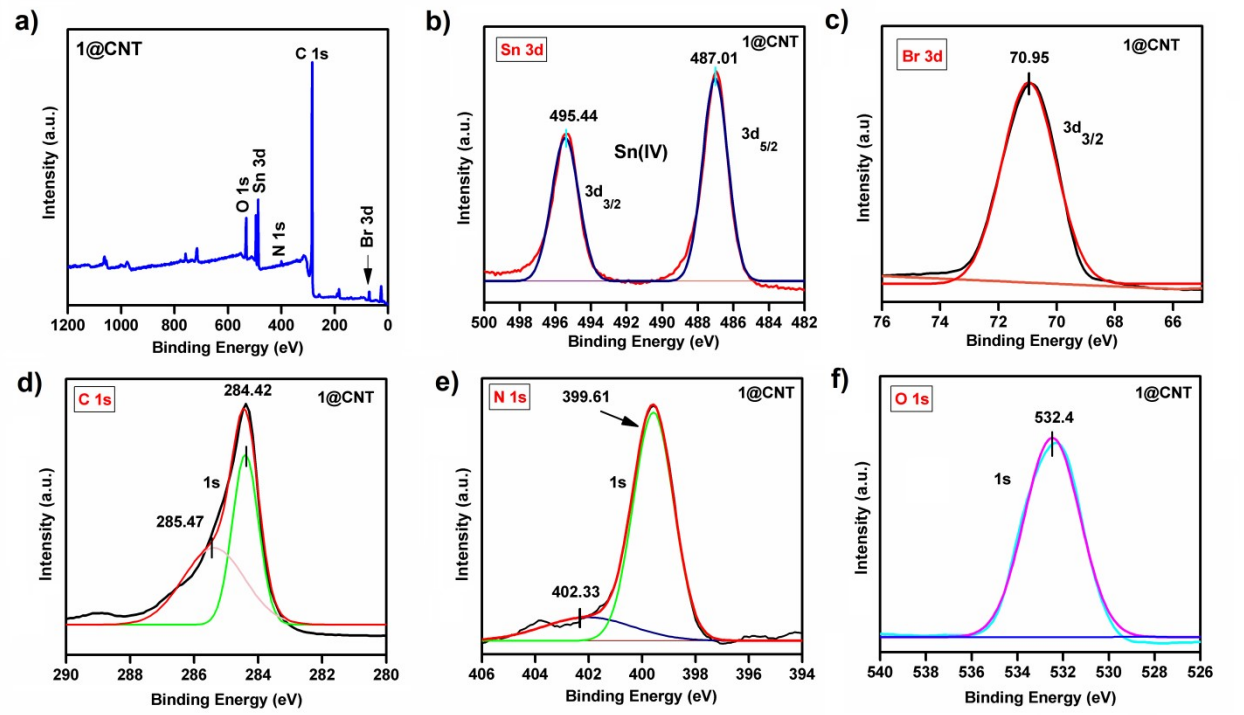

Fig. S38 Xps spectra of 1@CNT showing presence Sn 3d, Br 3d, C 1s, N 1s, and O 1s elements

.

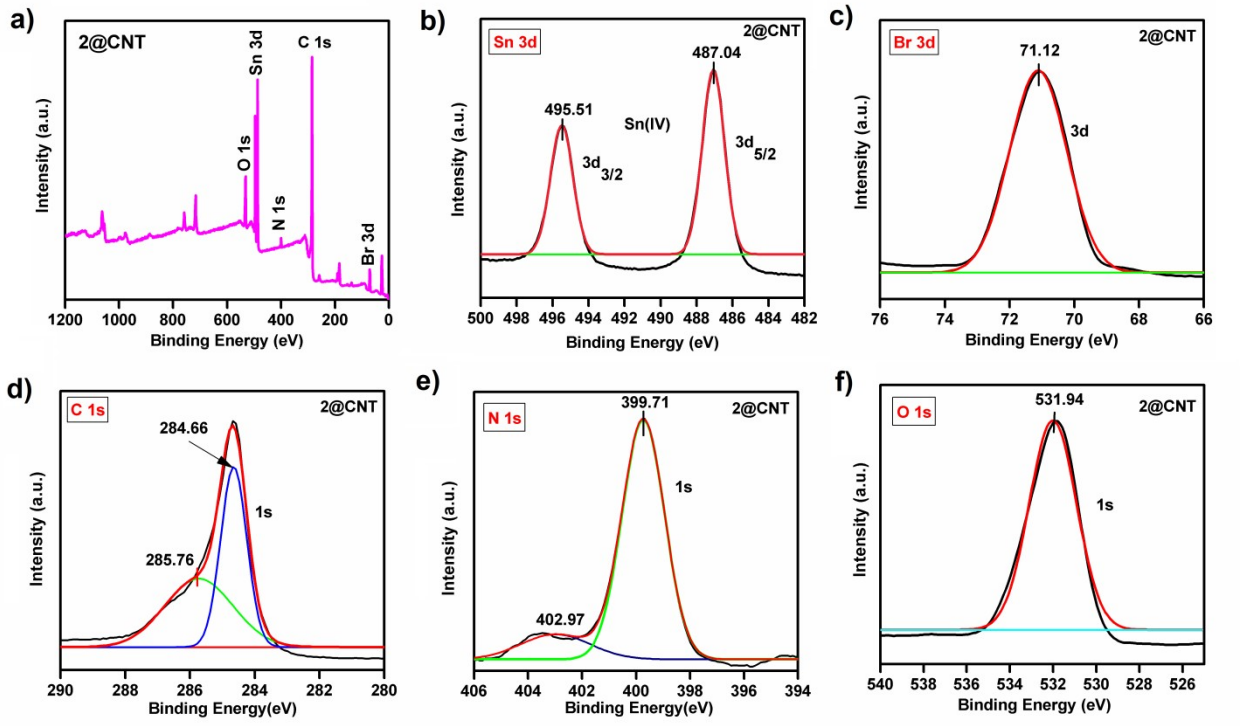

Fig. S39 Xps spectra of 2@CNT showing presence Sn 3d, Br 3d, C 1s, N 1s, and O 1s elements.

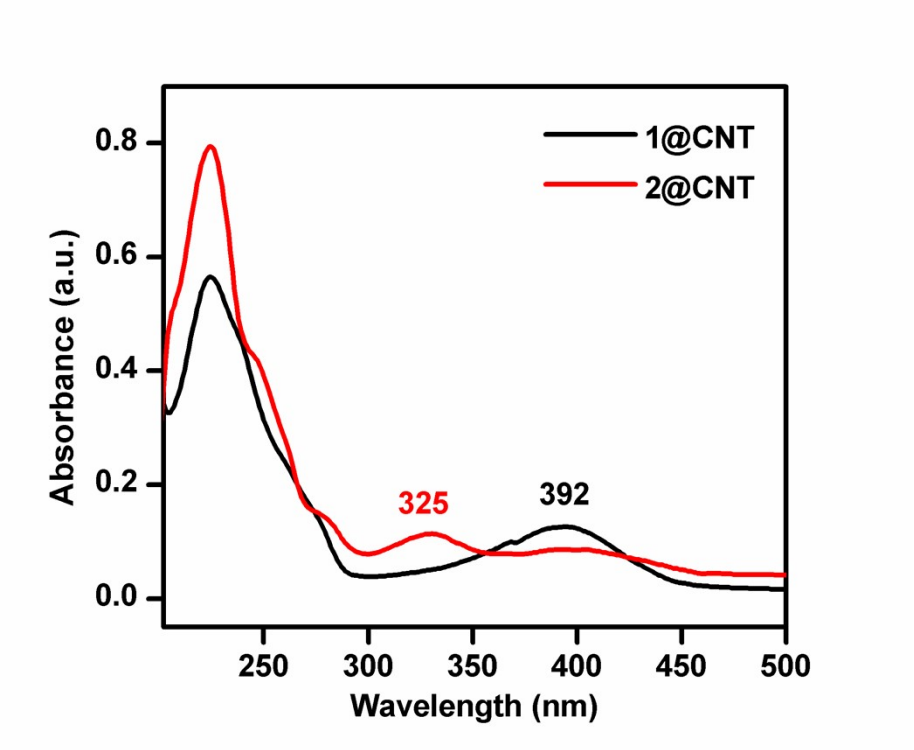

Fig. S40 UV absorption spectrum of 1@CNT and 2@CNT

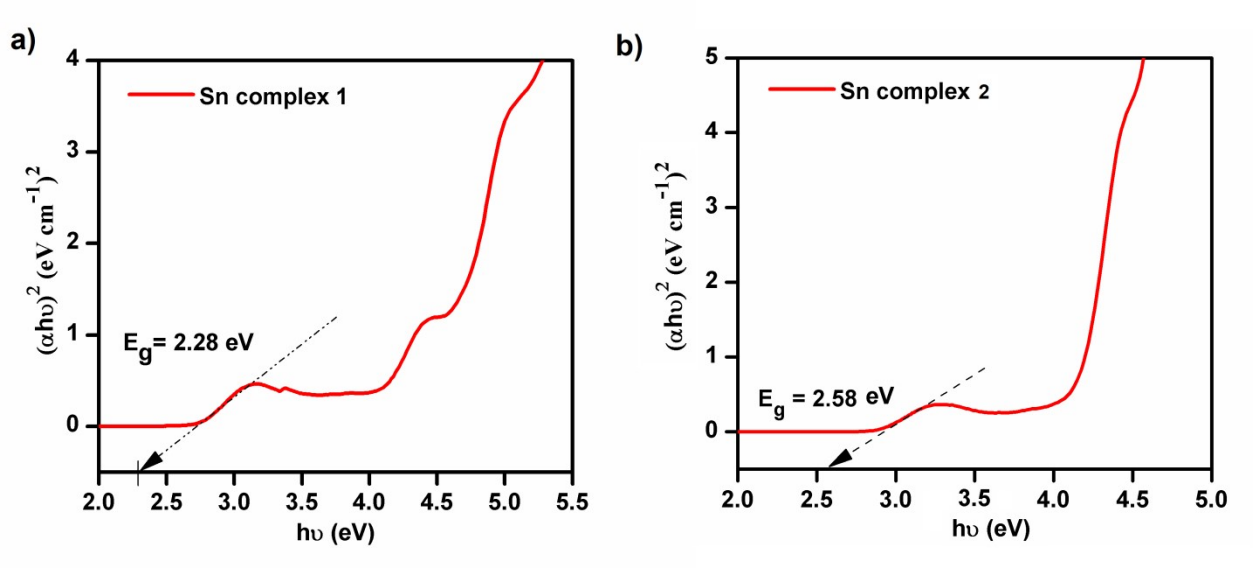

Fig. S41 Tauc plot of synthesized Sn complex 1 and 2, showing bandgap E_g

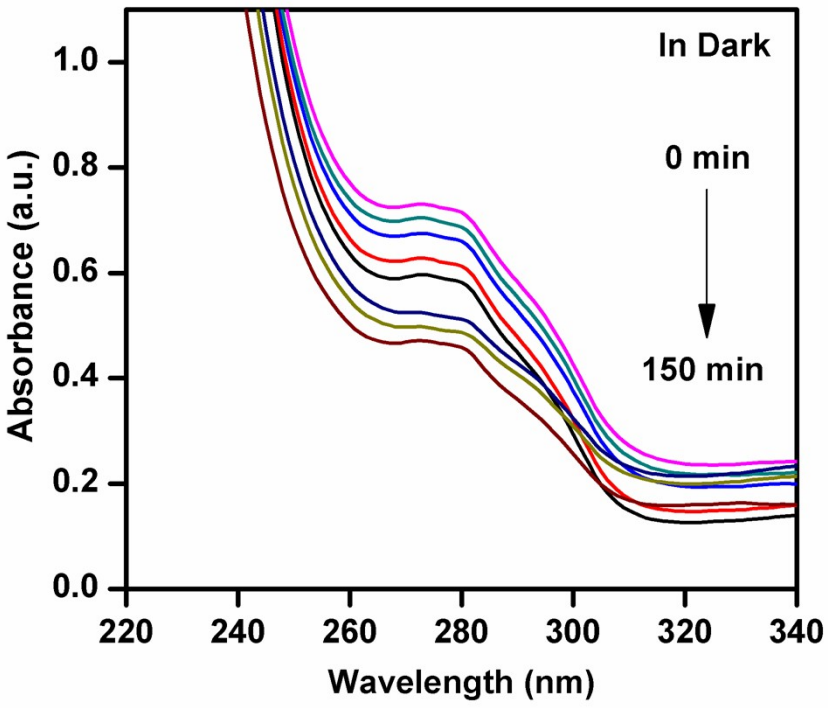

Fig. S42 Absorption spectra of AMX photocatalytic degradation under dark

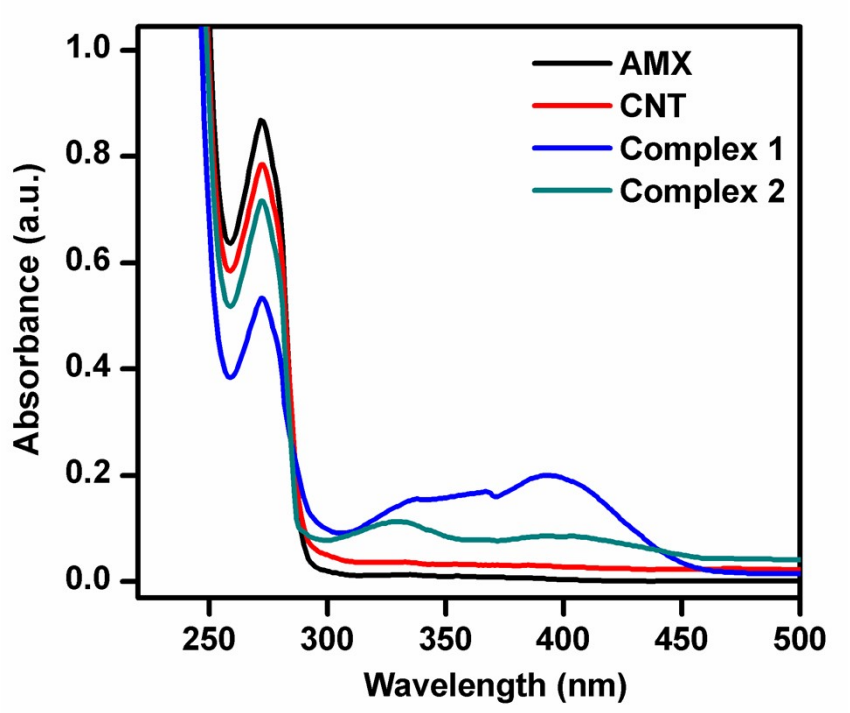

Fig. S43 Absorption spectra of AMX photocatalytic degradation using CNT, Complex 1, and Complex 2.

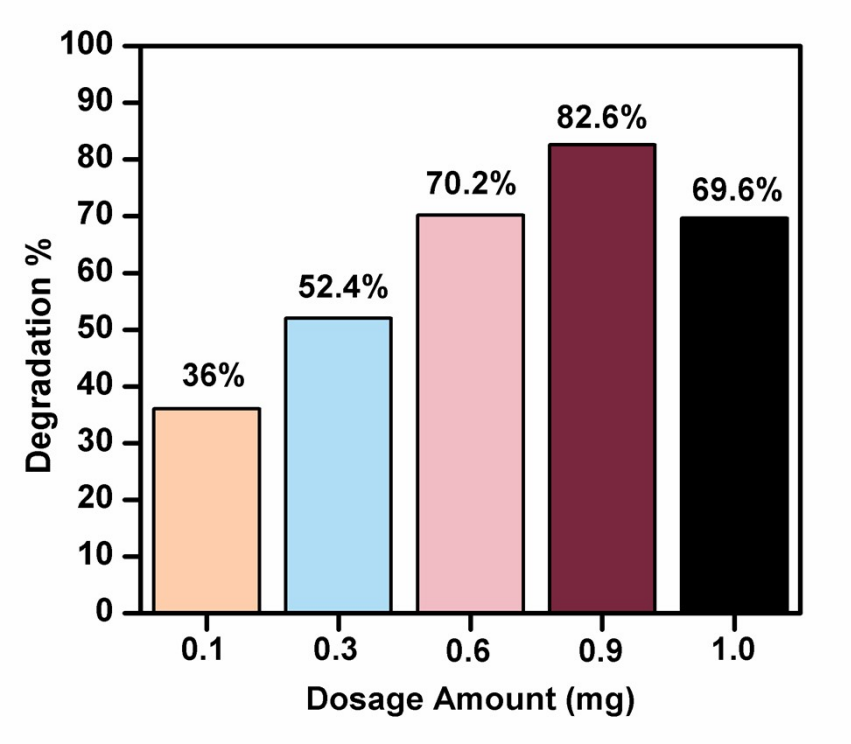

Fig. S44 Effect of dosage amount of 1@CNT on AMX degradation

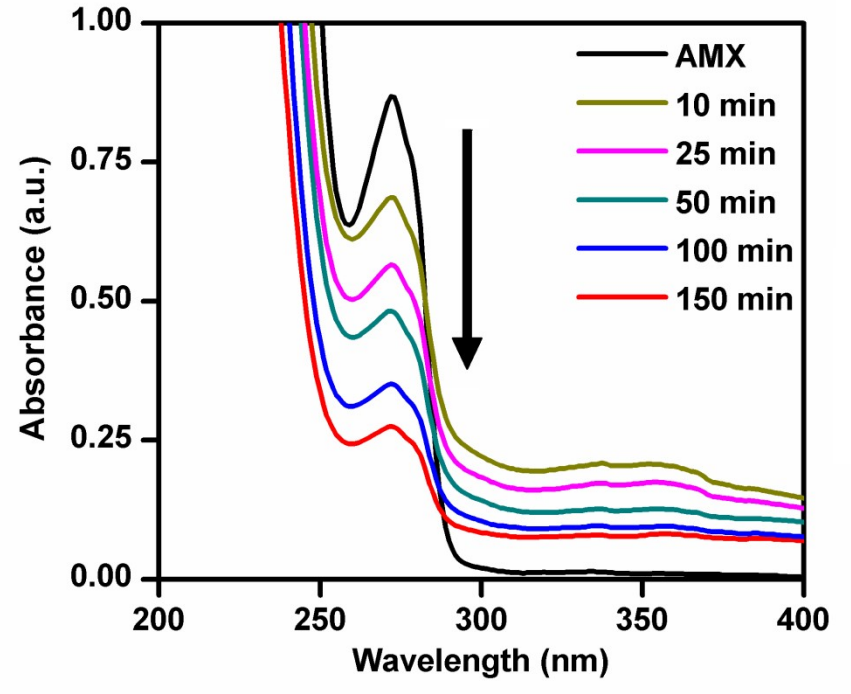

Fig. S45 Absorption spectra of AMX photocatalytic degradation using TiO2 as positive control.

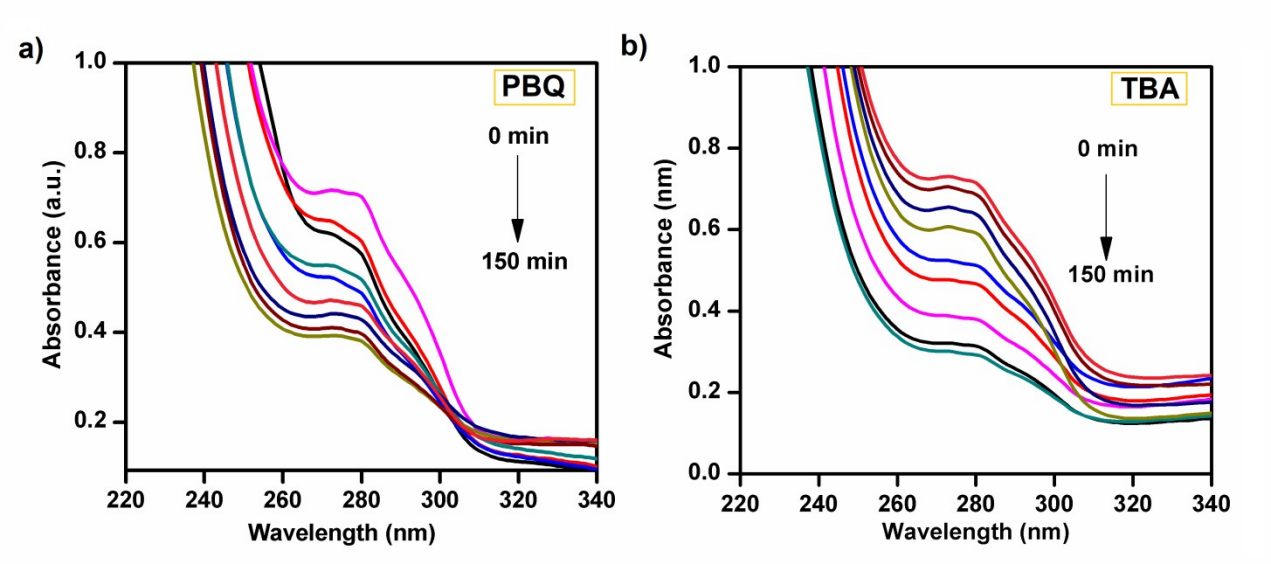

Fig. S46 Absorption spectra of AMX photocatalytic degradation under visible light irradiation in presence of radical scavengers a) p-benzoquinone (PBQ) and b) tertbutyl alcohol (TBA).

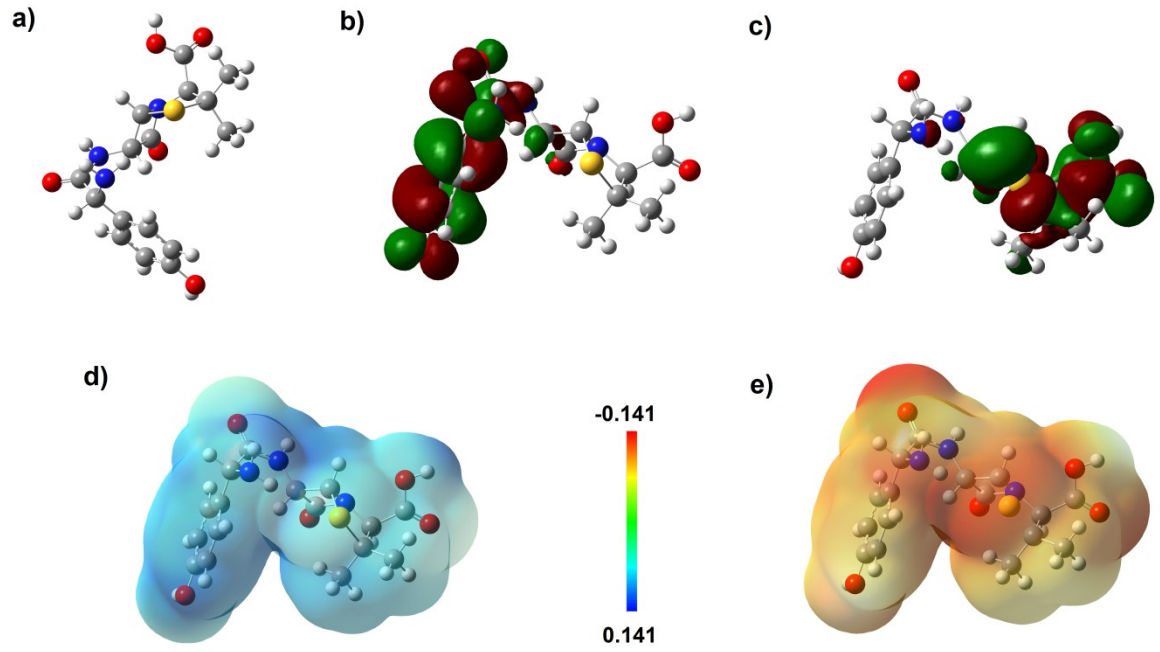

Fig. S47 a) DFT optimized structure of Amoxicillin using basis set 6-31g+(d,p), DFT calculated **b)** HOMO and **c)** LUMO molecular orbitals, Electrostatic potential (ESP) of Fukui function for **d)** nucleophilic attack (F^+) and e) electrophilic attack (F^-).

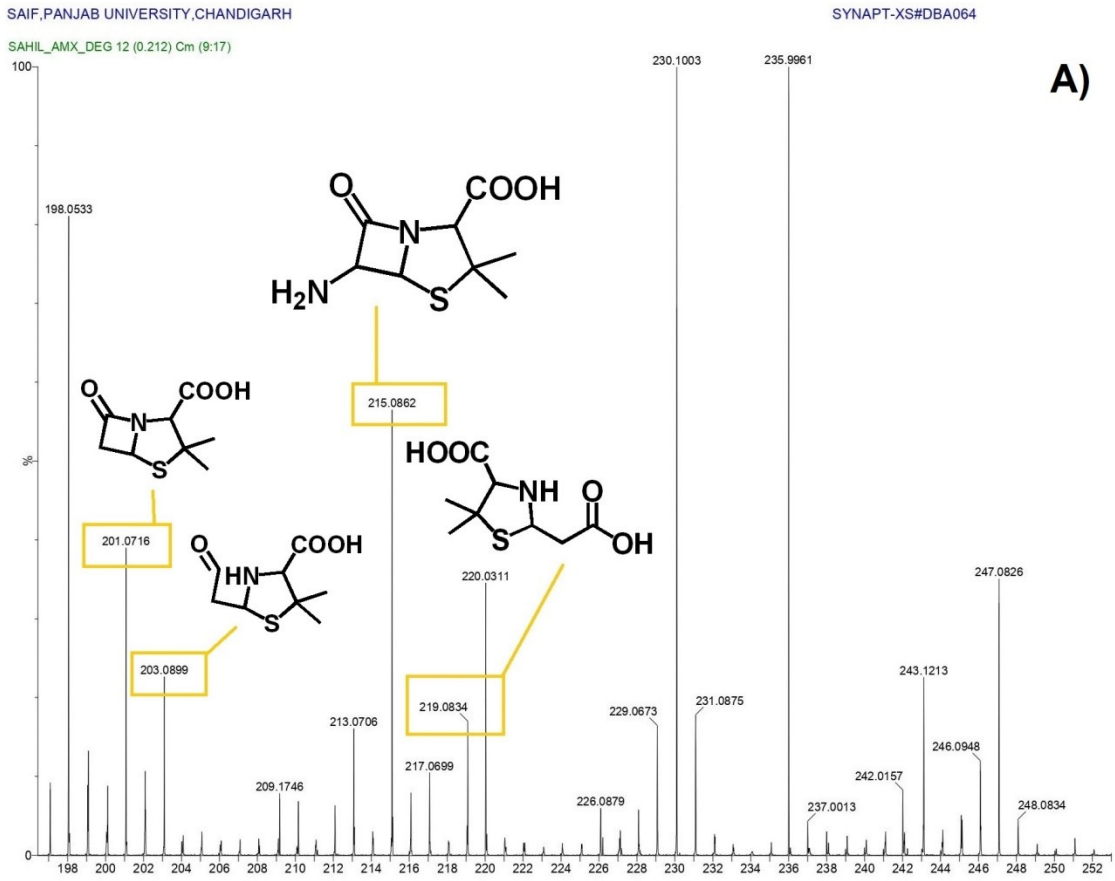
SAIF,PANJAB UNIVERSITY,CHANDIGARH
SYNAPT-XS#DBA064
SAHIL_AMX_DEG 12 (0.212) Cm (9:17)
A)
230.1003
235.9961
198.0533
215.0862
201.0716
220.0311
247.0826
203.0899
219.0834
243.1213
229.0673
231.0875
213.0706
246.0948
217.0699
242.0157
209.1746
226.0879
237.0013
248.0834
%
100
0
198 200 202 204 206 208 210 212 214 216 218 220 222 224 226 228 230 232 234 236 238 240 242 244 246 248 250 252

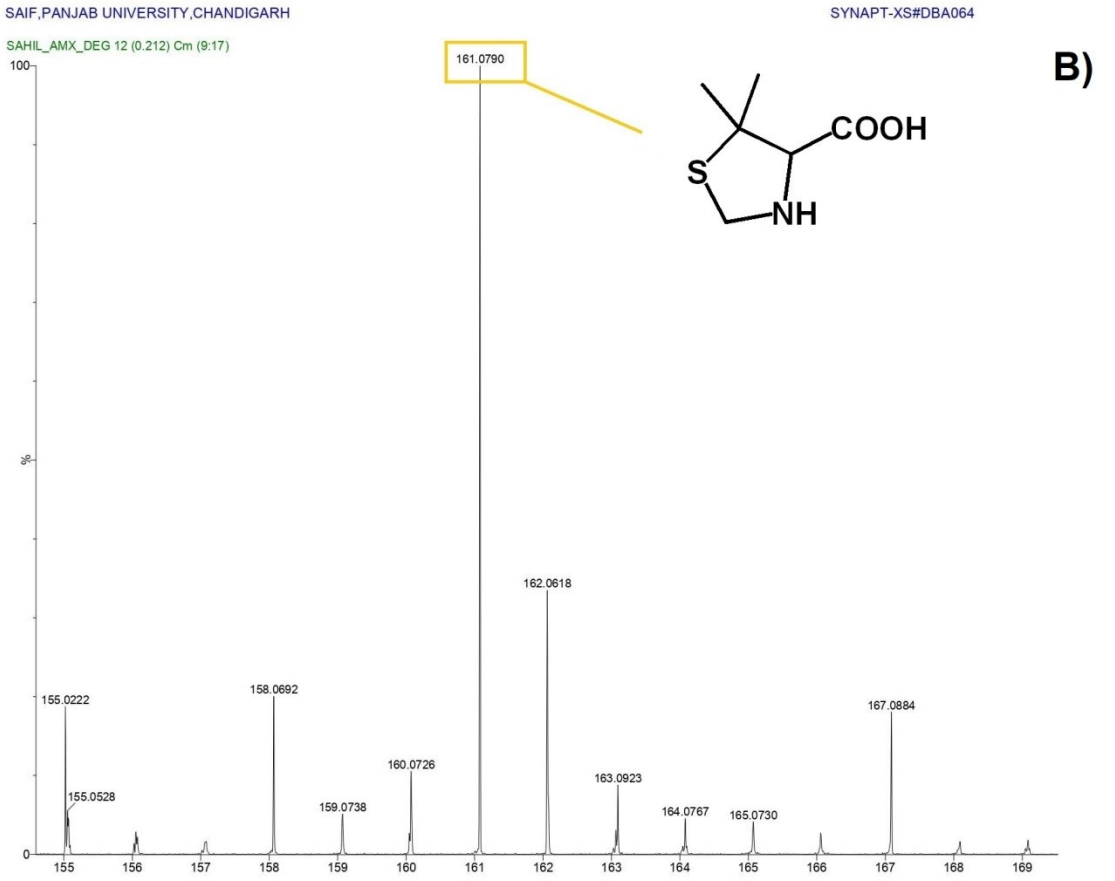
SAIF,PANJAB UNIVERSITY,CHANDIGARH
SYNAPT-XS#DBA064
SAHIL_AMX_DEG 12 (0.212) Cm (9:17)
B)
161.0790
162.0618
155.0222
158.0692
167.0884
160.0726
155.0528
163.0923
159.0738
164.0767
165.0730
%
100
0
155 156 157 158 159 160 161 162 163 164 165 166 167 168 169

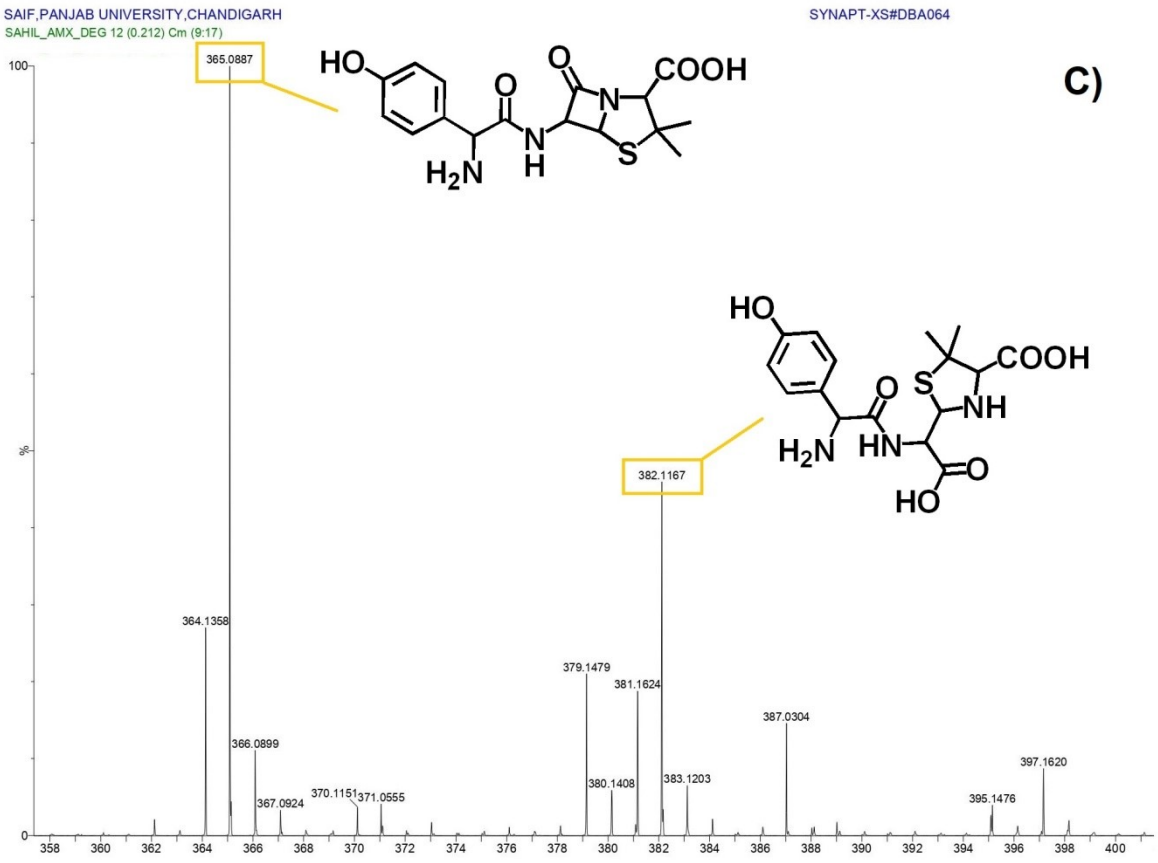
SAIF,PANJAB UNIVERSITY,CHANDIGARH
SYNAPT-XS#DBA064
SAHIL_AMX_DEG 12 (0.212) Cm (9:17)
C)
365.0887
382.1167
364.1358
366.0899
367.0924
370.1151
371.0555
379.1479
380.1408
381.1624
383.1203
387.0304
395.1476
397.1620

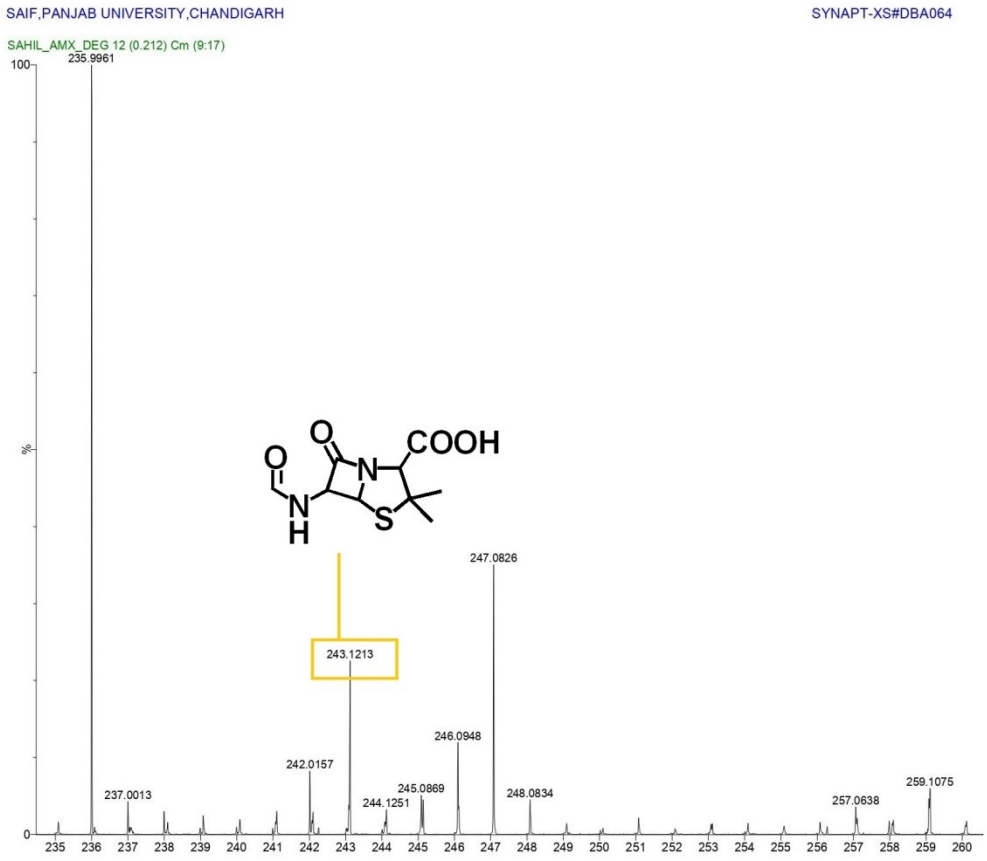
SAIF,PANJAB UNIVERSITY,CHANDIGARH
SYNAPT-XS#DBA064
SAHIL_AMX_DEG 12 (0.212) Cm (9:17)
D)
235.9961
237.0013
242.0157
243.1213
244.1251
245.0869
246.0948
247.0826
248.0834
257.0638
259.1075

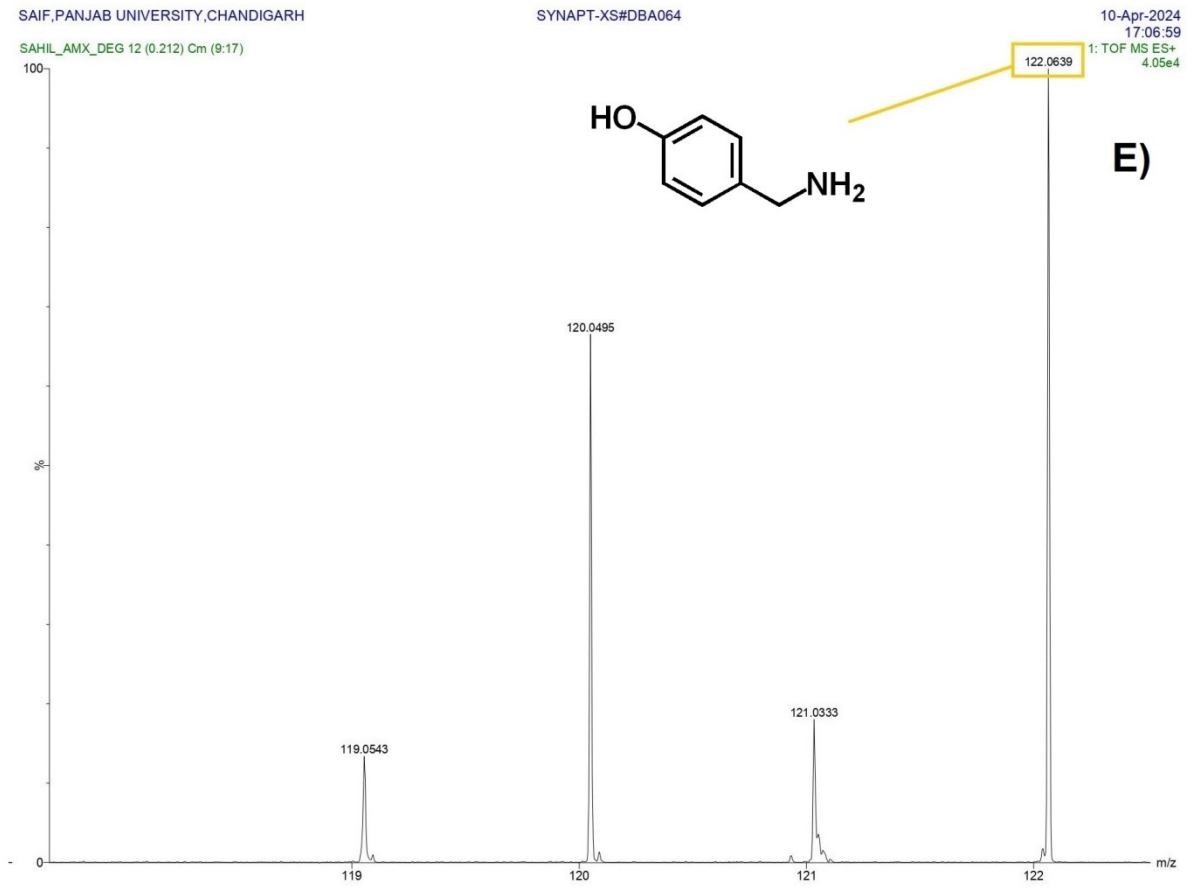

Fig. S48 AMX degradation products by HPLC-MS (A-E)

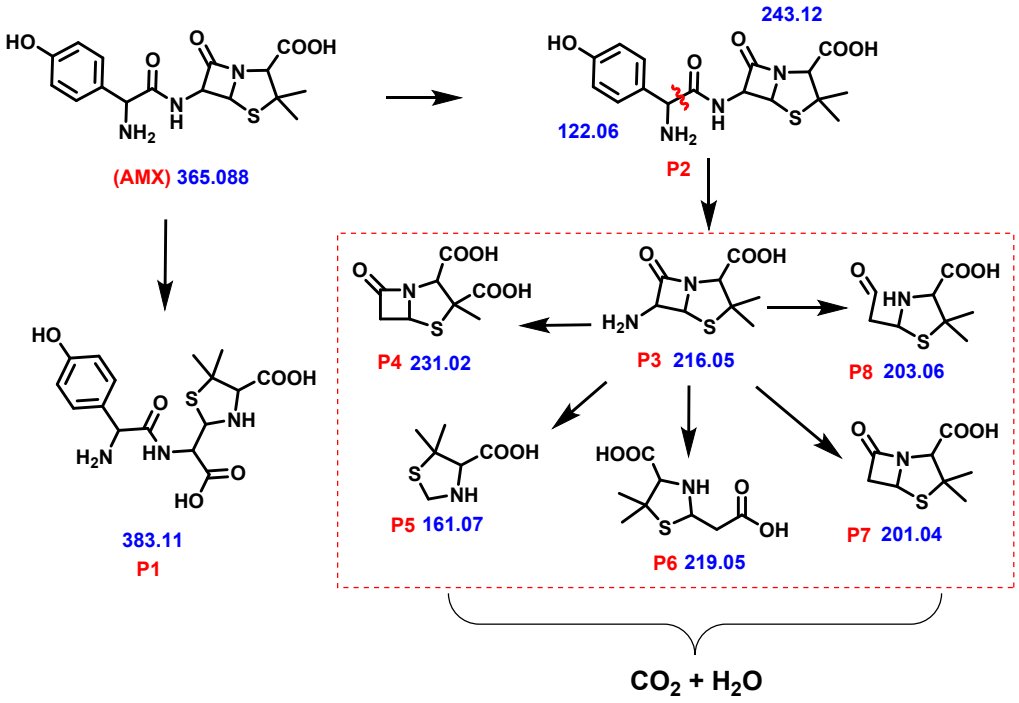

Fig. S49 Proposed degradation pathway of AMX.

Table S1 Crystallographic data and structural parameters for Ligands BSAL-EA and BSAL-DAP, Complexes 1 and 2.

PARAMETERS	**BSAL-EA**	**BSAL-DAP**	**Complex 1**	**Complex 2**
Empirical formula	$C_9H_{10}BrNO_2$	$C_{17}H_{16}Br_2N_2O_3$	$C_{24}H_{34}Br_2N_2O_6Sn_2$	$C_{28}H_{29}Br_3N_2O_5Sn_2$
Formula weight	244.09	456.14	843.73	950.64
Temperature/K	298	298	175(20)	236(100)
Crystal system	Monoclinic	Orthorhombic	Triclinic	Monoclinic
Space group	$P2_1/n$	$Pca2_1$	P-1	$P2_1/n$
a/Å	4.5073(2)	8.4537(6)	8.1743(3)	19.1383(15)
b/Å	11.5418(3)	6.1367(3)	9.9957(3)	20.8486(12)
c/Å	18.3112(6)	33.002(2)	10.3362(4)	28.771(2)
α/°	90	90	70.458(3)	90
β/°	96.065(3)	90	67.582(4)	97.455(7)
γ/°	90	90	72.878(3)	90
Volume/Å^3	947.26(6)	1712.09(18)	722.13(5	11382.7(14)
Z	4	4	1	12
ρ_{calc}g/cm^3	1.712	1.770	1.940	1.664
μ/mm^{-1}	4.305	4.753	4.535	4.508
F(000)	488.0	904.0	410.0	5472.0
Crystal size/mm^3	0.24 × 0.08 × 0.06	0.14 × 0.08 × 0.04	0.12 × 0.08 × 0.04	0.08×0.06×0.04
Radiation	Mo Kα (λ = 0.71073)	Mo Kα (λ = 0.71073)	Mo Kα (λ = 0.71073)	Mo Kα (λ = 0.71073)
2Θ range for data collection/°	7.06 to 54.146	6.64 to 50.102	6.35 to 54.766	6.22 to 56.942
Index ranges	$-5 \le h \le 5$, $-14 \le k \le 14$, $-22 \le l \le 23$	$-10 \le h \le 9$, $-7 \le k \le 7$, $-39 \le l \le 39$	$-10 \le h \le 10$, $-12 \le k \le 12$, $-13 \le l \le 11$	$-22 \le h \le 24$, $-25 \le k \le 25$, $-37 \le l \le 36$
Reflections collected	13911	13973	8754	110264
Independent reflections	2011 [R_{int} = 0.0455, R_{sigma} = 0.0318]	3007 [R_{int} = 0.0624 , R_{sigma} = 0.0670]	3037 [R_{int} = 0.0323 , R_{sigma} = 0.0447]	23251 [R_{int} = 0.3771 , R_{sigma} =

				0.3948]
Data/restraints/ parameter	2011/0/120	3007/1/219	3037/0/167	23251/0/1098
Goodness-of-fit on F^2	1.068	1.015	1.055	0.901
Final R indexes [I>=2σ (I)]	R_1 = 0.0425, wR_2 = 0.0918	R_1 = 0.0507, wR_2 = 0.1017	R_1 = 0.0334, wR_2 = 0.0822	R_1 = 0.1000, wR_2 = 0.2234
Final R indexes [all data]	R_1 = 0.0628, wR_2 = 0.0982	R_1 = 0.0873, wR_2 = 0.1134	R_1 = 0.0413, wR_2 = 0.0851	R_1 = 0.2813, wR_2 = 0.3092
Largest diff. peak/hole / e $Å^{-3}$	0.65/-0.39	0.28/-0.28	0.81/-0.74	1.38/-1.85

Table S2 Bonding parameters for for Ligands BSAL-EA and BSAL-DAP, Complexes 1 and 2.

Bond angles (°)							
BSAL-EA		**BSAL-DAP**		**Complex 1**		**Complex 2**	
C7-N1-C8	122.5 (3)	C3-N2-C2	119.7 (10)	O1-Sn1-O2[1]	139.41 (9)	O1-Sn1-O4	144.1 (4)
N1-C7-C5	123.1 (3)	C11-N1-C10	122.3 (10)	O2-Sn1-O1	150.64 (10)	O2-Sn1-O5	137.7 (4)
C6-C1-Br1	120.6 (3)	N2-C3-C4	122.3 (11)	O2-Sn1-O2[1]	69.60 (11)	O5-Sn1-O4	70.4 (4)
O1-C4-C5	120.9 (3)	C7-C8-Br2	120.5 (9)	O2-Sn1-N1	75.05 (10)	O2-Sn1-N1	70.3 (4)
O1-C4-C3	120.3 (3)	N2-C2-C1	111.6 (9)	N1-Sn1-O1	76.48 (10)	O2-Sn2-O3	151.9 (4)
N1-C8-C9	111.6 (3)	O2-C1-C2	111.7 (9)	C10-Sn1-N1	109.31 (15)	O2-Sn2-N2	73.8 (6)
O2-C9-C8	107.8 (3)	N10-C10-C1	110.9 (9)	C11-Sn1-N1	97.53 (15)	N2-Sn2-O4	143.9 (5)
Bond length (Å)							
BSAL-EA		**BSAL-DAP**		**Complex 1**		**Complex 2**	
Br1-C1	1.901(3)	Br1-C16	1.900 (11)	Sn1-O1	2.273 (3)	Sn1-O1	2.162 (12)
O1-C4	1.283(4)	Br2-C8	1.884 (11)	Sn1-O2	2.094 (2)	Sn1-O2	2.252 (12)
O2-C9	1.406(4)	O2-C1	1.399(12)	Sn1-N1	2.244 (3)	Sn1-N1	2.262 (12)
N1-C7	1.292(4)	O1-C13	1.280 (12)	Sn1-C10	2.101 (4)	Sn2-N2	2.243 (16)
N1-C8	1.458(4)	O3-C5	1.339 (13)	Sn1-C11	2.113 (4)	Sn2-O4	2.436 (11)
C7-C5	1.419(4)	N2-C3	1.272 (13)	Sn1-O2[1]	2.399 (2)	Sn2-O2	2.156 (12)

Table S3 charge distribution and Fukui index of AMX

Atom (number)	**Charge (0)** $(e/\overset{0}{A})$	**Charge (+1)** $(e/\overset{0}{A})$	**Charge (-1)** $(e/\overset{0}{A})$	f^+	f^-	f^0
C (1)	-0.220	-0.215	-0.222	0.005	0.002	0.0035
C (2)	-0.101	0.006	-0.100	0.107	-0.001	0.053
C (3)	-0.217	-0.194	-0.257	0.023	0.04	0.0315
C (4)	-0.306	-0.272	-0.319	0.034	0.013	0.0235
C (5)	0.313	0.380	0.292	0.067	0.021	0.044
C (6)	-0.282	-0.223	-0.222	0.059	-0.06	-0.0005
O (11)	-0.712	-0.622	-0.726	0.09	0.014	0.052
C (13)	-0.174	-0.190	-0.196	-0.016	0.022	0.003
C (18)	0.686	0.678	0.674	-0.008	0.012	0.002
O (19)	-0.623	-0.529	-0.659	0.094	0.036	**0.065**
N (15)	-0.909	-0.851	-0.959	0.058	0.05	**0.054**
N (20)	-0.677	-0.653	-0.674	0.024	-0.003	0.0105
C (22)	-0.166	-0.160	-0.178	0.006	0.012	0.009
C (23)	-0.194	-0.207	-0.221	-0.013	0.027	0.007
O (28)	-0.566	-0.521	-0.626	0.045	0.06	**0.0525**
C (27)	0.711	0.707	0.665	-0.004	0.046	0.021
N (26)	-0.504	-0.0482	-0.0520	0.022	0.016	0.019
C (29)	-0.162	-0.166	-0.164	-0.004	0.002	-0.001
C (40)	0.826	0.818	0.752	-0.008	-0.074	0.033
O (41)	-0.596	-0.568	-0.674	0.028	0.078	**0.053**
O (42)	-0.722	-0.726	-0.744	-0.004	0.022	0.009
C (31)	-0.176	-0.169	-0.211	0.007	0.035	0.021
C (32)	-0.708	-0.716	-0.700	-0.008	-0.008	-0.008
C (36)	-0.699	-0.702	-0.696	-0.003	-0.003	**-0.003**
S (44)	0.170	0.287	0.053	0.117	0.117	0.117